DNA-dependent ATPase and chromatin-remodeling activities (9–15). Recent studies suggested that Rad54 may play diverse roles in multiple stages of homologous recombination (16,17). Rad54 promotes and stabilizes the Rad51–ssDNA nucleoprotein filament formation by physically interacting with Rad51 (18–21), and it also stimulates the homologous pairing and strand-exchange reactions mediated by Rad51 (22–25). These facts suggest that Rad54 functions in the early stage of homologous recombination. Rad54 is also known to disassemble Rad51 nucleoprotein filaments from DNA, which may be essential in the later stages of recombination (26). Moreover, Rad54 promotes branch migration of the Holliday junction in an ATP-dependent manner, suggesting that Rad54 functions in the late stage of recombination (25).

RAD54B, which shares homology with Rad54, was identified in the human cell as a member of the SWI2/SNF2 family proteins (27). Like Rad54, RAD54B is a DNA-dependent ATPase and stimulates the RAD51-mediated homologous pairing (28,29). Previously, our group and others reported that RAD54B stimulates the recombination activity of DMC1, a meiosis-specific RAD51 homolog, suggesting its role in meiotic homologous recombination (30–32). Therefore, Rad54B may be a paralog of Rad54 having both overlapping and non-overlapping roles with those of Rad54. RAD54B contains helicase motifs, which are commonly found in the members of the SWI2/SNF2 family. Outside this region, RAD54B has an N-terminal region of ~300 amino acid residues. The corresponding region in RAD54 directly interacts with RAD51 (19), suggesting that the N-terminal region of RAD54B may also be essential for the interactions with other recombination factors. However, the N-terminal region of RAD54B is considerably longer than that of RAD54. Hence, it is of interest whether the N-terminal region of RAD54B contains functional regions that are not present in that of RAD54. In the present study, we identified a stable N-terminal domain of the human RAD54B protein, and found that this domain is capable of self-associating, binding to DNA and interacting with both RAD51 and DMC1. These observations suggest multifunctional roles of the N-terminal domain of RAD54B in homologous recombination.

MATERIALS AND METHODS

Purification of RAD54B$_{26-225}$

The His$_6$-tagged human RAD54B$_{26-225}$ protein was overexpressed in the *Escherichia coli* JM109 (DE3) strain carrying an expression vector for the minor tRNAs [Codon(+)RIL, (Novagen, Darmstadt, Germany)], using the pET15b expression system (Novagen). Harvested cells were disrupted by sonication in buffer A (pH 7.8), containing 50 mM Tris–HCl, 0.3 M KCl, 2 mM 2ME, 10% glycerol and 5 mM imidazole. Lysates were mixed gently by the batch method with 4 ml Ni-NTA beads at 4°C for 1 h. The RAD54B$_{26-225}$-coupled Ni-NTA agarose beads were then packed into an Econo-column (Bio-Rad Laboratories, Hercules, CA, USA) and were washed with 30 CV of buffer B (pH 7.8), which contained 50 mM Tris–HCl, 0.3 M KCl, 2 mM 2ME, 10% glycerol and 20 mM imidazole. The His$_6$-tagged RAD54B$_{26-225}$ was eluted in a 30 CV linear gradient of 20–300 mM imidazole in buffer B. RAD54B$_{26-225}$, which eluted in a broad peak, was collected and treated with 2 U of thrombin protease (GE Healthcare, Biosciences, Uppsala, Sweden) per milligram of RAD54B$_{26-225}$. The RAD54B$_{26-225}$ protein was then dialyzed against buffer C (pH 7.2), which contained 20 mM HEPES–KOH, 0.1 M KCl, 0.5 mM EDTA, 2 mM 2ME and 10% glycerol, and was mixed with 2 ml of Benzamidine-Sepharose (GE Healthcare) column matrix at 4°C for 1 h. The proteins in the Benzamidine-Sepharose flow-through fraction were mixed with 8 ml of Q-Sepharose column matrix at 4°C for 1 h. The proteins in the Q-Sepharose flow-through fraction were then mixed with 8 ml of SP-Sepharose column matrix at 4°C for 1 h. The SP-Sepharose column was washed with 20 CV of buffer C, and the RAD54B$_{26-225}$ protein was eluted with a 20 CV linear gradient from 0.1 to 1.0 M KCl in this buffer. The peak fractions of the RAD54B$_{26-225}$ proteins were collected, dialyzed against buffer D (pH 7.5), which contained 20 mM HEPES–KOH, 0.1 M KCl, 0.5 mM EDTA, 2 mM 2ME and 10% glycerol, and stored at −80°C.

Purification of the DMC1 deletion mutants

Ten overlapping glutathione *S*-transferase (GST)-fused DMC1 deletion mutants, composed of amino acid residues 1–44, 24–66, 47–104, 84–126, 118–162, 153–214, 195–237, 225–270, 264–306 and 296–340, respectively, were overexpressed in the *E. coli* JM109 (DE3) strain carrying an expression vector for the minor tRNAs [Codon(+)RIL], using the pET41b expression system (Novagen). The cells were suspended in buffer E (pH 8.0), containing 50 mM Tris–HCl, 0.3 M KCl, 2 mM 2ME, 5 mM EDTA and 10% glycerol, and were disrupted by sonication. Lysates were mixed gently by the batch method with 500 µl Glutathione Sepharose 4B (GS4B) beads (GE Healthcare) at 4°C for 1 h. The beads bound with the GST–DMC1 deletion mutants were then washed four times with 10 ml of buffer E. The GST–DMC1 deletion mutants were eluted by 1 ml of buffer E with 20 mM glutathione. These proteins were dialyzed against buffer E and were stored at 4°C.

The RAD51 and DMC1 proteins were purified as described previously (30,33,34). The concentrations of the purified proteins were determined with a Bio-Rad protein assay kit, using BSA as the standard.

DNA substrates

The φX174 circular ssDNA and replicative form I DNA were purchased from New England Biolabs, Ipswich, MA, USA and Life Technologies, Gaithersburg, MD, USA. The concentrations of these DNA are expressed as molar nucleotide concentrations. The oligonucleotides used in this study are shown in Table 1. They were purchased from Invitrogen, Carlsbad, CA, USA, in the desalted form, and were purified by anion exchange

Table 1. Oligonucleotides used in this study

Name	Length	Sequence (5′ to 3′)
PolyA	44-mer	AAAAAAAAAAAAAAAAAAAAAAAAAAAAAAAAAAAAAAAAAAAA
2	50-mer	TGGGTCAACGTGGGCAAAGATGTCCTAGCAATGTAATCGTCTATGACGTT
2a	50-mer	AACGTCATAGACGATTACATTGCTAGGACATCTTTGCCCACGTTGACCCA
5	50-mer	TGCCGAATTCTACCAGTGCCAGTGATGGACATCTTTGCCCACGTTGACCC
6	50-mer	GTCGGATCCTCTAGACAGCTCCATGATCACTGGCACTGGTAGAATTCGGC
7	50-mer	CAACGTCATAGACGATTACATTGCTACATGGAGCTGTCTAGAGGATCCGA
8	51-mer	CAACGTCATAGACGATTACATTGCTAATCACTGGCACTGGTAGAATTCGGC
10	24-mer	GGACATCTTTGCCCACGTTGACCC
15	26-mer	TGCCGAATTCTACCAGTGCCAGTGAT

chromatography. Briefly, the oligonucleotides were dissolved in water and applied to a MonoQ column (GE Healthcare) equilibrated with 10 mM NaOH. Oligonucleotides 2, 2a, 5, 6, 7 and 8 were eluted in a two-step linear gradient, consisting of 5 column volumes of 0–0.6 M NaCl followed by 50 column volumes of 0.6–0.9 M NaCl. Oligonucleotides 10 and 15 were also eluted in a two-step linear gradient, consisting of 5 column volumes of 0–0.5 M NaCl followed by 50 column volumes of 0.5–0.8 M NaCl. Peak fractions were collected, ethanol precipitated and dissolved in water. The substrates with various structures were made by annealing appropriate combinations of oligonucleotides, as described previously (35–37). The combinations of oligonucleotides were as follows: dsDNA, oligonucleotides 2 and 2a; Splayed arm, oligonucleotides 2 and 8; 3′-tailed duplex, oligonucleotides 2 and 10; 5′-tailed duplex, oligonucleotides 8 and 15; 3′-flapped DNA, oligonucleotides 2, 8 and 10; 5′-flapped DNA, oligonucleotides 2, 8 and 15; 3′-PX junction, oligonucleotides 2, 6, 7 and 10; 5′-PX junction, oligonucleotides 2, 6, 7 and 15; and X junction, oligonucleotides 2, 5–7. Oligonucleotide substrates are expressed as molar molecule concentrations.

Gel filtration analysis of $RAD54B_{26-225}$

$RAD54B_{26-225}$ was concentrated to 5.6 mg/ml and 50 µl of the concentrated protein was fractionated through a 25 ml Superdex 200 10/30 GL column (GE Healthcare) using buffer G.

DNA-binding assays of $RAD54B_{26-225}$

For the plasmid DNA-binding assay, the indicated amounts of $RAD54B_{26-225}$ were incubated with ϕX174 ssDNA (20 µM) or ϕX174 dsDNA (10 µM) at 37°C for 20 min in 10 µl of buffer H, containing 50 mM Tris–HCl (pH 7.8), 100 µg/ml BSA and 1mM DTT. After 10-fold loading dye was added, the products were resolved by 1% agarose gel electrophoresis in TAE buffer at 3.3 V/cm for 2.5 h, and were visualized by staining with ethidium bromide. For the binding assays using oligonucleotide substrates, the indicated amounts of $RAD54B_{26-225}$ were incubated with the DNA substrates (0.2 µM) at 37°C in 10 µl of buffer H for either 10 min for ssDNA or 20 min for other substrates. $A^{32}P$-labeled polyA oligonucleotide was used as the ssDNA substrate, and the resulting $RAD54B_{26-225}$–polyA complex was resolved by 1% agarose gel electrophoresis in 0.5 × TBE buffer at 3.3 V/cm for 2 h. The gel was dried, exposed to an imaging plate and visualized using a BAS2500 image analyzer (Fuji Film Co., Tokyo, Japan). For other DNA substrates containing various structures, the complexes with $RAD54B_{26-225}$ were resolved by 5% polyacrylamide gel electrophoresis in 1 × TBE buffer at 100 V for 50 min, and were visualized by staining with ethidium bromide.

Protein–protein binding assay of $RAD54B_{26-225}$

$RAD54B_{26-225}$ was covalently conjugated to Affi-Gel 15 beads (100 µl, Bio-Rad), according to the manufacturer's instructions. The unbound proteins were removed by washing the beads five times with binding buffer F (pH 7.5), which contained 20 mM HEPES–KOH, 0.15 M KCl, 0.5 mM EDTA, 2 mM 2ME, 10% glycerol and 0.05% Triton X-100. To block the residual active ester sites, ethanolamine (pH 8.0) was added to a final concentration of 100 mM and the resin was incubated at 4°C overnight. After washing the resin five times with 500 µl of buffer F, the Affi-Gel 15-protein matrices were adjusted to 50% slurries with buffer F and were stored at 4°C. For the binding assay, 20 µl of the Affi-Gel 15-protein slurry were mixed with 20 µg of RAD51, DMC1 or RecA at room temperature for 2 h. The Affi-Gel 15-protein beads were then washed five times with 500 µl of buffer F. SDS–PAGE sample buffer (2-fold) was mixed directly with the washed beads. After heating the mixture at 98°C for 5 min, the proteins were fractionated by 12% SDS–PAGE. Bands were visualized by Coomassie Brilliant Blue staining.

In the GS4B pull-down assay, GS4B beads (30 µl) were equilibrated with buffer G, containing 20 mM Tris–HCl (pH 8.0), 0.2 M KCl, 2 mM 2ME, 5 mM EDTA, 10% glycerol and 0.1% NP-40, and were mixed with 10 µg of the GST–DMC1 deletion mutants at 4°C for 30 min. To prevent nonspecific interactions between $RAD54B_{26-225}$ and the GS4B beads, the GS4B–DMC1 deletion mutants were first incubated with 500 µg/ml BSA, and the reaction was incubated at 4°C for 30 min, followed by the addition of 10 µg of $RAD54B_{26-225}$. After an incubation at 4°C for 1 h, the GS4Bbeads were washed with buffer G five times and were eluted with SDS–PAGE sample buffer.

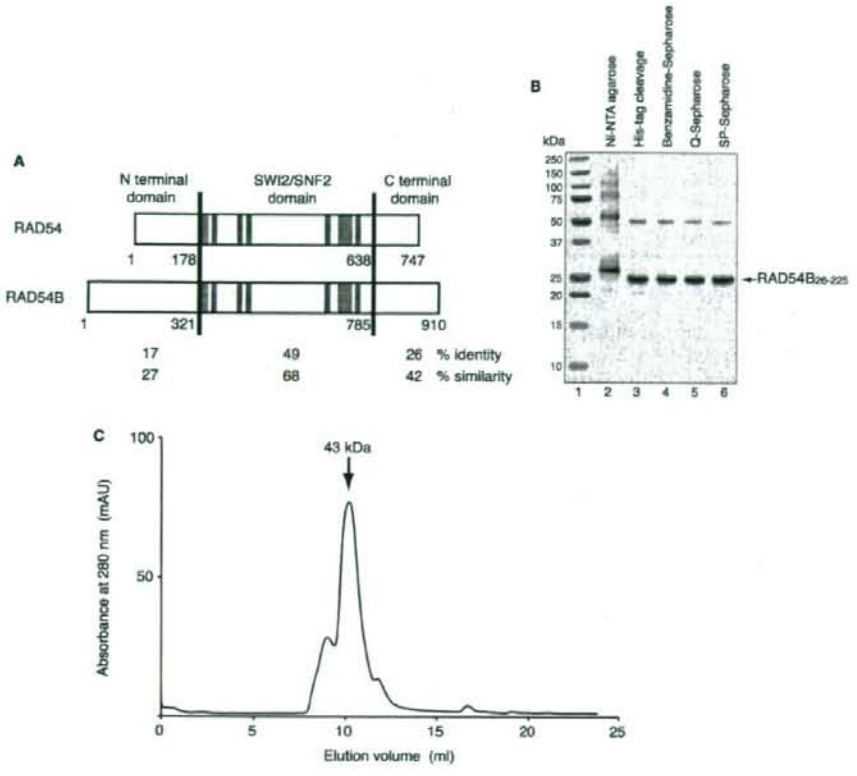

Figure 1. (**A**) Sequence comparison of RAD54 and RAD54B. These proteins are separated into three regions (N-terminal domain, SWI2/SNF2 domain and C-terminal domain), and the amino acid sequence identities and similarities between these proteins were calculated for each region. The amino acid number at the boundary of each domain is denoted. The gray lines indicate the seven helicase motifs (I, Ia, II, III, IV, V and VI, respectively). (**B**) Purification of the $RAD54B_{26-225}$ protein. The peak fractions from the Ni-NTA agarose column (lane 2), the fraction after the removal of the His_6 tag (lane 3), the Benzamidine Sepharose flow-through (lane 4), the Q-Sepharose flow-through (lane 5) and the peak fractions from the SP-Sepharose column (lane 6) were analyzed on a 12% SDS–PAGE gel, which was stained with Coomassie Brilliant Blue. Lane 1 indicates the molecular mass markers. (**C**) Gel filtration analysis of $RAD54B_{26-225}$. The arrow indicates the peak location of a molecular weight marker, ovalbumin (43 kDa), which nearly corresponds to that of $RAD54B_{26-225}$.

ssDNA- and dsDNA-binding assays of DMC1

The indicated amounts of DMC1 were incubated with ϕX174 ssDNA (20 μM) or ϕX174 dsDNA (10 μM) at 37°C for 20 min in 10 μl of buffer I, containing 50 mM Tris–HCl (pH 7.8), 1 mM ATP, 2 mM $MgCl_2$, 100 μg/ml BSA and 1 mM DTT. After 10-fold loading dye was added, the products were resolved by 1% agarose gel electrophoresis in TAE buffer at 3.3 V/cm for 2.5 h, and were visualized by staining with ethidium bromide.

Interaction between DMC1 and $RAD54B_{26-225}$ on ssDNA and dsDNA

The reactions were started by incubating 40 μM DMC1 with 20 μM ϕX174 ssDNA or 10 μM ϕX174 dsDNA at 37°C for 20 min, in 10 μl of buffer I. The indicated amounts of $RAD54B_{26-225}$ were then incorporated, and the mixtures were incubated at 37°C for 20 min. After 10-fold loading dye was added, the products were resolved by 1% agarose gel electrophoresis in TAE buffer at 3.3 V/cm for 2.5 h. To determine whether DMC1 was present, the protein–DNA complex was localized by ethidium bromide staining of the agarose gel, and the corresponding area of the gel was excised for electroelution. The eluted proteins were fractionated by 12% SDS–PAGE, and the bands were visualized by Coomassie Brilliant Blue staining.

RESULTS

Purification of the RAD54B N-terminal domain fragment

To gain insight into the function of the N-terminal region of RAD54B, which is less conserved between RAD54 and RAD54B (Figure 1A), we constructed a RAD54B deletion mutant containing the first 295 residues ($RAD54B_{1-295}$).

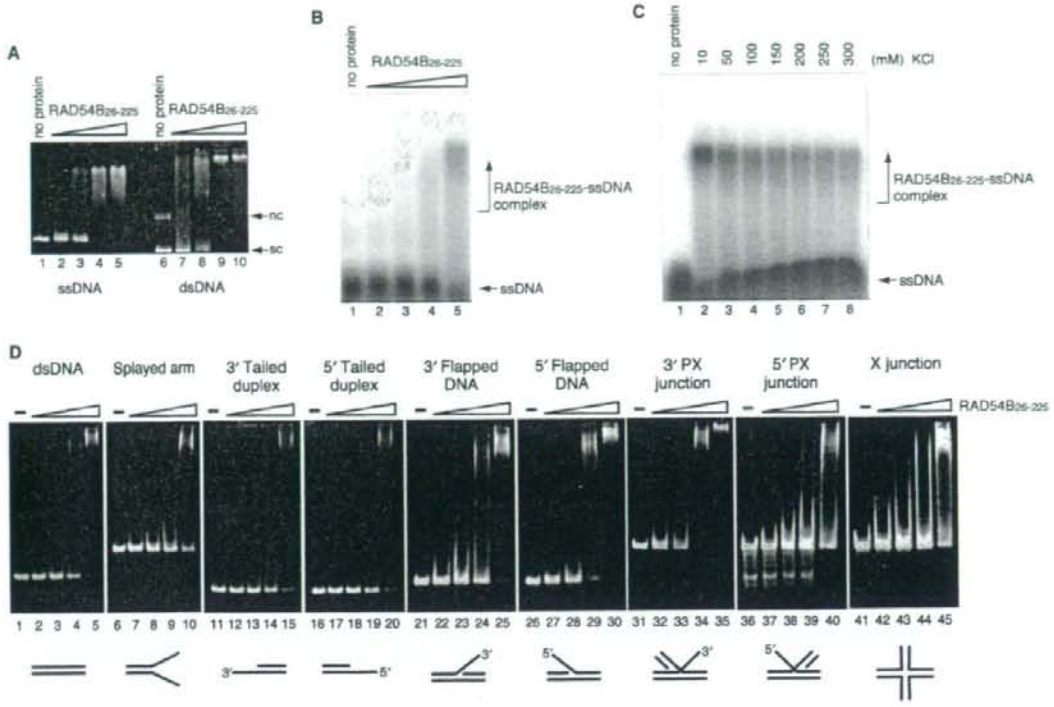

Figure 2. DNA-binding activity of $RAD54B_{26-225}$. (**A**) Plasmid ssDNA (20 μM in nucleotides, lanes 1–5) or plasmid superhelical dsDNA (10 μM in nucleotides, lanes 6–10) was incubated with $RAD54B_{26-225}$ at 37°C for 20 min. The concentrations of $Rad54B_{26-225}$ used in the DNA-binding experiments were 2.0 μM (lanes 2 and 7), 4.0 μM (lanes 3 and 8), 8.0 μM (lanes 4 and 9) and 16 μM (lanes 5 and 10). The reaction mixtures were fractionated on a 1% agarose gel, which was stained with ethidium bromide. Nc and sc indicate nicked circular and superhelical dsDNA, respectively. (**B**) A ^{32}P labeled single-stranded oligonucleotide (polyA 44-mer, 0.2 μM in molecules) was incubated with $RAD54B_{26-225}$ (2, 4, 8 or 16 μM) at 37°C for 10 min and the reaction mixtures were fractionated on a 1% agarose gel. (**C**) Salt concentration titration for the $RAD54B_{26-225}$–polyA complex. $RAD54B_{26-225}$ (16 μM) was incubated with a ^{32}P labeled single-stranded oligonucleotide (polyA 44-mer, 0.2 μM in molecules) in the reaction mixture containing the indicated concentrations of KCl. The reaction mixtures were fractionated on a 1% agarose gel. (**D**) Various branched DNA substrates (0.2 μM in molecules) were incubated with $RAD54B_{26-225}$ (2, 4, 8 or 16 μM) at 37°C for 20 min, and the reaction mixtures were fractionated on a 5% polyacrylamide gel, which was stained with ethidium bromide.

However, this fragment rapidly degraded to several smaller fragments during the expression and purification processes, suggesting that the fragment contained unstructured or flexible regions. Several rounds of fragment design and purification were performed to identify the stable N-terminal region of RAD54B. We found that the fragment consisting of amino acid residues 26–225 of RAD54B ($RAD54B_{26-225}$) was resistant to proteolysis and was highly soluble. The $RAD54B_{26-225}$ mutant was expressed in the *E. coli* JM109 (DE3) strain, as a fusion protein with an N-terminal His_6 tag containing a cleavage site for thrombin protease, and was purified by Ni-NTA column chromatography (Figure 1B, lane 2). After the His_6 tag was uncoupled with thrombin protease (Figure 1B, lane 3), the peak fractions containing $RAD54B_{26-225}$ were further purified by Benzamidine column chromatography (Figure 1B, lane 4), Q-Sepharose column chromatography (Figure 1B, lane 5) and SP-Sepharose column chromatography (Figure 1B, lane 6). About 10 mg of purified $RAD54B_{26-225}$ were obtained from 2.5 l of *E. coli* suspension culture. The SDS–PAGE analysis of the final purification fraction revealed an additional band with an apparent molecular weight of about 50 kDa. The band disappeared when higher concentrations of reducing agent were included in the electrophoresis sample buffer, indicating that $RAD54B_{26-225}$ oligomerizes. Consistent with this observation, a gel filtration analysis of the purified $RAD54B_{26-225}$ indicated that the fragment primarily exists as a dimer (Figure 1C). These results demonstrated that amino acid residues 26–225 of RAD54B form a stable domain. Although it is not known whether the full-length RAD54B protein multimerizes, the N-terminal region may play a role in the self-association of RAD54B.

DNA-binding activity of $RAD54B_{26-225}$

The conserved region of RAD54B (amino acid residues 321–785) contains the helicase motifs involved in DNA binding. As expected, the full-length RAD54B has both

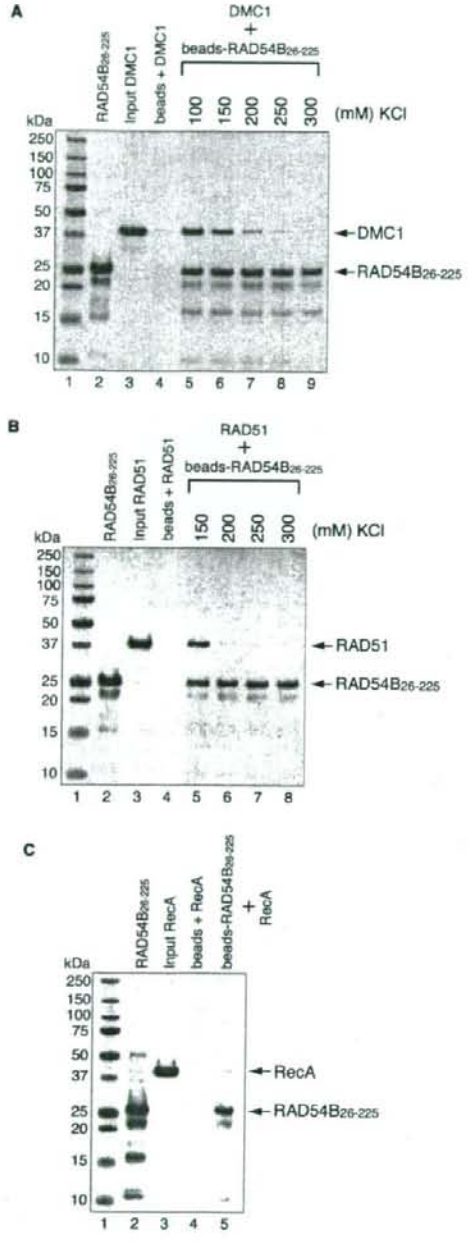

Figure 3. $RAD54B_{26-225}$ interacts with RAD51 and DMC1. The interactions were observed by a pull-down assay, in which DMC1 (**A**) or RAD51 (**B**) was mixed with $RAD54B_{26-225}$ that was covalently conjugated to an Affi-Gel 15 matrix. The proteins bound to the $RAD54B_{26-225}$-conjugated beads were eluted by SDS–PAGE sample buffer, and fractionated on a 12% SDS–PAGE gel. Lanes 2 and 3 are one-tenth of the total proteins used. Lane 4 is the negative control using the Affi-Gel 15 matrix without $RAD54B_{26-225}$. The salt concentration was titrated for both binding experiments, which are shown beyond lane 5. (**C**) Interaction between bacterial RecA and $RAD54B_{26-225}$. The binding experiment was performed in the presence of 100 mM KCl. The bands were visualized by Coomassie Brilliant Blue staining.

ssDNA- and dsDNA-binding activities (28). In contrast, the less conserved N-terminal domain of RAD54B has no known DNA-binding motifs, and it is not known whether this domain binds to DNA. Therefore, we first examined the DNA-binding activity of $RAD54B_{26-225}$, using plasmid ssDNA and dsDNA substrates. As shown in Figure 2A, $RAD54B_{26-225}$ bound to both plasmid ssDNA and dsDNA. To further characterize the DNA-binding activity of $RAD54B_{26-225}$, oligonucleotide substrates were used. $RAD54B_{26-225}$ bound to a polyA ssDNA oligonucleotide, a substrate that is free of secondary structures (Figure 2B). The binding was observed at higher salt concentrations (Figure 2C), suggesting that $RAD54B_{26-225}$ interacts with ssDNA through specific interactions and not by nonspecific ionic interactions. $RAD54B_{26-225}$ also interacted with a dsDNA oligonucleotide, as well as DNA oligonucleotides with branched structures (Figure 2D). The binding experiments were performed using the same concentrations of the DNA substrates (0.2 μM) and RAD54B (2, 4, 8 and 16 μM), to facilitate comparisons between the results with different DNA substrates. We found that $RAD54B_{26-225}$ exhibited slightly higher affinity for dsDNA than ssDNA (compare the amount of uncomplexed DNA between Figure 2B, lane 5 and 2D, lane 5). This was also apparent from the higher affinity for dsDNA than for DNA substrates with shorter duplex regions, such as the splayed arm and the 3′-tailed or 5′-tailed duplexes (Figure 2D, lanes 1–20). We also found that among the branched DNA substrates we tested, $RAD54B_{26-225}$ displayed the highest affinity for 5′-flapped DNA and 3′-PX junction (Figure 2D, lanes 26–35). These results suggested that $RAD54B_{26-225}$ may specifically function on branched DNA molecules.

$RAD54B_{26-225}$ interacts with both RAD51 and DMC1

We have previously shown that RAD54B interacts with RAD51 and DMC1 (30). However, it is not known whether the N-terminal domain of RAD54B is involved in the interactions. We therefore tested the interactions between the N-terminal domain of RAD54B and RAD51 or DMC1 by a pull-down assay, using $RAD54B_{26-225}$-conjugated Affi-Gel 15 beads. The proteins bound to the $RAD54B_{26-225}$ beads were detected by SDS–PAGE. Consistent with the fact that $RAD54B_{26-225}$ self-associates (Figure 1C), we observed $RAD54B_{26-225}$ in the elution fraction that was not covalently conjugated to the Affi-Gel beads (Figure 3A, lanes 5–9; 3B, lanes 5–8 and 3C, lane 5). As shown in Figures 3A and B, $RAD54B_{26-225}$ interacted with both RAD51 and DMC1 (Figure 3A, lanes 5–9 and 3B, lanes 5 and 6, respectively). In contrast, $RAD54B_{26-225}$ weakly bound to RecA, the bacterial homolog of RAD51 and DMC1, suggesting that the interactions between $RAD54B_{26-225}$ and RAD51 or DMC1 were specific (Figure 3C). When the salt concentrations

were titrated for the RAD51- and DMC1-binding experiments, the amounts of RAD51 and DMC1 bound to $RAD54B_{26-225}$ sharply decreased at 200 mM of KCl (Figure 3A, lane 7 and 3B, lane 6). In the case of DMC1, the binding was observed even at 300 mM of KCl, whereas the RAD51 binding was absent at 250 mM of KCl. This difference in binding affinities could reflect the differences in the mechanisms of interactions between $RAD54B_{26-225}$ and RAD51 or DMC1.

Interaction of $RAD54B_{26-225}$ with ssDNA- and dsDNA-bound DMC1

We next addressed whether $RAD54B_{26-225}$ can interact with the DMC1 protein bound to either ssDNA or dsDNA. To do this, DMC1–DNA complexes were initially formed, followed by the addition of $RAD54B_{26-225}$ and the resulting complexes were examined by a gel shift assay. To minimize the chance of $RAD54B_{26-225}$ binding to the DMC1-free regions of the DNA molecule, we determined the concentrations of DMC1 required to nearly saturate the DNA substrates (Figure 4A, lanes 4 and 9). These concentrations of DMC1 were incubated with ssDNA or dsDNA, followed by the addition of $RAD54B_{26-225}$ to the reaction mixture. As shown in Figure 4B (lanes 3–6 and lanes 10–13), increasing concentrations of $RAD54B_{26-225}$ resulted in the supershifting of the DMC1–DNA complexes in the agarose gel. The supershifted complexes migrated differently from the $RAD54B_{26-225}$–DNA complex (Figure 4B, lanes 7 and 14). These results indicated that $RAD54B_{26-225}$ can form ternary complexes with DMC1 and either ssDNA or dsDNA. In the experiments shown in Figure 4B (lanes 13 and 14), the migration distances of the DMC1–$RAD54B_{26-225}$–dsDNA ternary complex and the $RAD54B_{26-225}$–dsDNA complex were nearly the same. To exclude the possibility that DMC1 had dissociated from the DNA, leaving behind the $RAD54B_{26-225}$–dsDNA complex, we performed an electroelution of the protein–DNA complex, to investigate whether it contained DMC1. As confirmed by SDS–PAGE, both DMC1 and $RAD54B_{26-225}$ were detected (Figure 4C), indicating that the DMC1–$RAD54B_{26-225}$–dsDNA ternary complex was actually formed.

Identification of the DMC1 region that binds to $RAD54B_{26-225}$

Previously, we found that RAD54B interacts with the ATPase domain of DMC1. To define more precisely the regions of DMC1 that interact with RAD54B, 10 DMC1 fragments were designed to cover the entire region of the DMC1 sequence (Figure 5A). These fragments were expressed as GST-fused proteins. The GST-fused DMC1 fragments required a short induction time and rapid purification. Otherwise, the fragments readily degraded to a size of about 25 kDa, which is likely GST. Even with careful purification, partial degradation products were observed with some of the DMC1 fragments (Figure 5B, lanes 3, 4, 5, 7–9). A pull-down assay using GS4B beads was carried out (Figure 5B). In this assay, $RAD54B_{26-225}$ was pulled down with GST-fused DMC1 fragments

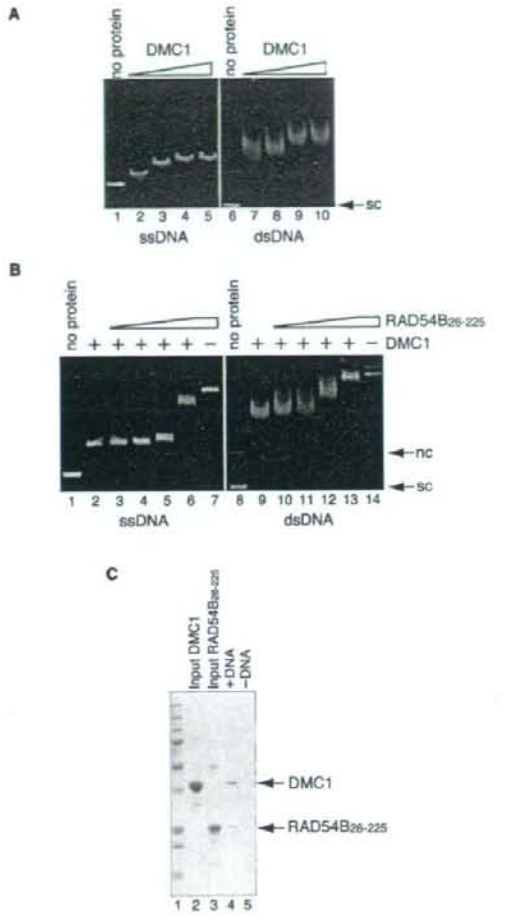

Figure 4. Interaction between DMC1 and $RAD54B_{26-225}$ on DNA. (**A**) DNA-binding activity of DMC1. Increasing amounts of DMC1 (10, 20, 40 and 80 μM in lanes 2–5 and lanes 7–10, respectively) were incubated with ϕX174 ssDNA (20 μM in nucleotides) or ϕX174 superhelical dsDNA (10 μM in nucleotides). Lanes 1 and 6 indicate negative control experiments without protein. The reaction mixtures were fractionated on a 1% agarose gel, which was stained with ethidium bromide. (**B**) $RAD54B_{26-225}$ forms ternary complexes with DMC1 and DNA. A constant amount of DMC1 (40 μM) was incubated with ϕX174 circular ssDNA (20 μM in nucleotides) or ϕX174 superhelical dsDNA (10 μM in nucleotides) at 37°C for 20min, followed by an incubation with increasing amounts of $RAD54B_{26-225}$ (0, 2.0, 4.0, 8.0 and 16 μM in lanes 2–6 and lanes 9–13, respectively) at 37°C for 20 min. In lanes 7 and 14, $RAD54B_{26-225}$ (16 μM) was incubated with ssDNA and dsDNA, but not DMC1, respectively. Lanes 1 and 8 indicate negative control experiments without protein. (**C**) Electroelution analysis of the protein–DNA complex. The protein–DNA complex detected in Figure 4B lane 13 was electroeluted from the agarose gel, and was analyzed by 12% SDS–PAGE gel (lane3). Lane 5 is the negative control experiment performed without dsDNA. Lane 1 indicates the molecular mass markers. *Lanes 2 and 3* are one-tenth of the input DMC1 and $RAD54B_{26-225}$, respectively. Nc and sc indicate nicked circular and superhelical dsDNA, respectively.

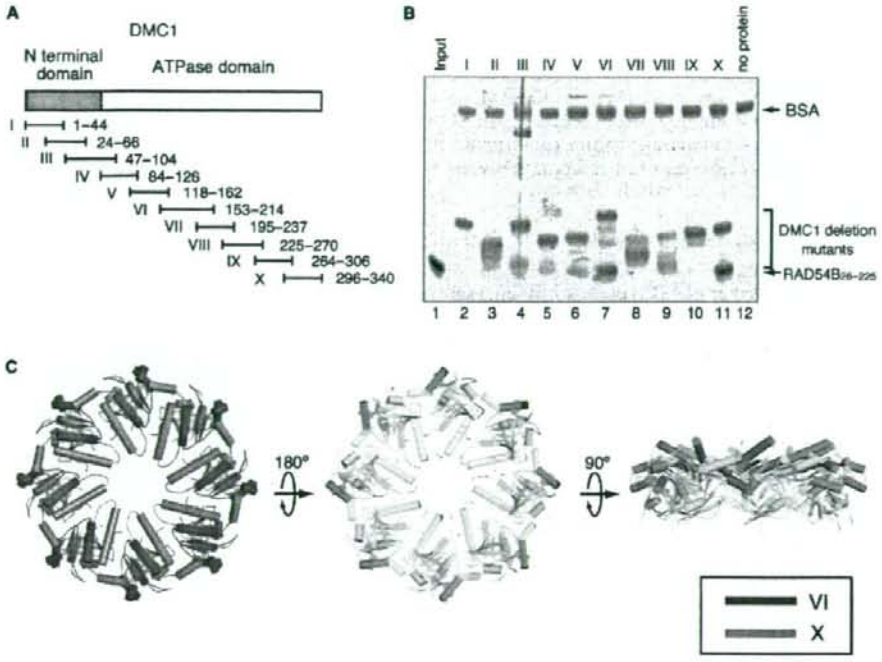

Figure 5. (**A**) A schematic representation of the 10 overlapping GST–DMC1 fusion proteins. The gray bar indicates the N-terminal domain of DMC1, and the white bar indicates the core ATPase domain. (**B**) Protein–protein interaction assay of $RAD54B_{26-225}$ with the DMC1 deletion mutants. The GS4B–DMC1 deletion mutant beads were first mixed with BSA, to prevent nonspecific protein binding, followed by the addition of $RAD54B_{26-225}$. After an incubation at 4°C for 1 h, the GS4B–DMC1 deletion mutant beads were washed with binding buffer. The $RAD54B_{26-225}$ proteins that bound to the GS4B–DMC1 deletion mutant beads were fractionated by 12% SDS–PAGE gel (lanes 2–11, respectively). Lane 1 is one-tenth of the input proteins, and lane 12 is the negative control experiment using the GS4B beads without the DMC1 deletion mutant. (**C**) The $RAD54B_{26-225}$-binding sites mapped on the DMC1 octameric ring. The purple region indicates $DMC1_{153-214}$, and the yellow region indicates $DMC1_{296-340}$.

bound to GS4B beads, and was detected by SDS–PAGE. As shown in Figure 5B, $RAD54B_{26-225}$ bound to DMC1 fragments VI and X, and weakly to V (Figure 5B, lanes 6, 7 and 11), but did not bind to other fragments. Regions VI and X are located close to each other and are exposed on the surface of the crystal structure of DMC1 (Figure 5C). The $RAD54B_{26-225}$ bound to DMC1 fragments VI and X with relatively high affinity, and these DMC1 fragments were relatively stable, suggesting that the interactions are specific.

DISCUSSION

Several studies have indicated that RAD54B and Rad54 have similar biochemical properties (29,30,38,39). To clarify the similarities and differences between RAD54B and Rad54, we focused on the poorly characterized N-terminal region of RAD54B, which shares less conservation with the corresponding region in RAD54. We found a stable domain of RAD54B that is composed of amino acid residues 26–225. This region seems to be absent in RAD54, as no structured domains were found outside the crystal structure of the core region of the zebrafish Rad54 protein (amino acid residues 91–738; Figure 1A; see Ref. 40).

The $RAD54B_{26-225}$ fragment self-associates and exists primarily as a dimer in solution. We also found that the $RAD54B_{26-225}$ fragment has both ssDNA- and dsDNA-binding activities. Among the branched DNA substrates tested, $RAD54B_{26-225}$ exhibited the highest affinities for 5′-flapped DNA and 3′-PX junction. Interestingly, cross-linking studies of the RAD54 protein demonstrated that the fundamental unit of this protein is a dimer (41). Furthermore, the RAD54 protein preferentially binds to branched DNA substrates, with the highest preference for PX junction (42). These activities are proposed to be the basis for the specific recognition of the branched DNA substrate by oligomeric RAD54 (42). Our result suggested that RAD54B may similarly self-associate on DNA, and that the N-terminal region could provide important interactions for the oligomerization and the DNA binding.

The $RAD54B_{26-225}$ fragment also physically interacted with both the RAD51 and DMC1 recombinases. Previously, we demonstrated that RAD54B stimulates the DMC1-mediated strand exchange by stabilizing the

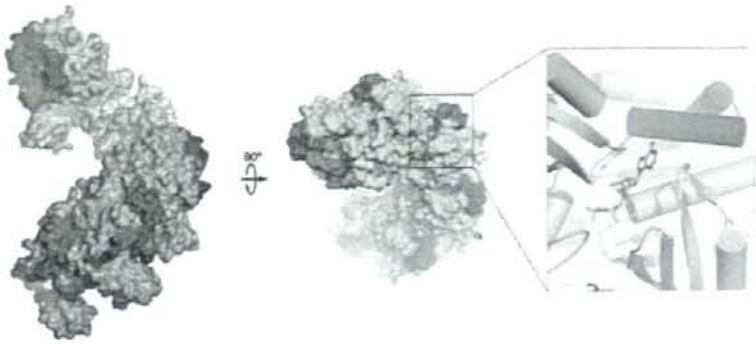

Figure 6. Proposed orientations of the $RAD54B_{26-225}$-interacting regions of DMC1 in the helical filament form. DMC1 sites essential for the interaction with $RAD54B_{26-225}$ were mapped on the corresponding locations of the *M. voltae* RadA filament. The closeup view shows the ATP-binding site that is surrounded by the $RAD54B_{26-225}$-interacting regions. All structural figures were prepared using the PyMOL program (44).

DMC1–ssDNA complex, and proposed that RAD54B may promote the formation of the active DMC1 helical filament (30). In this study, we found that $RAD54B_{26-225}$ bound to both DMC1 alone and DMC1 complexed with DNA, and we mapped the RAD54B-interacting regions of DMC1 (amino acid residues 153–214 and 296–340). These regions are exposed on the surface of the octameric ring. The corresponding regions in the *Methanococcus voltae* RadA protein, a homolog of DMC1 that forms a helical filament (43), are also exposed on the surface. Thus, the RAD54B-interacting regions appear to be easily accessible by other factors, in both the ring and helical filament forms. These regions, for example, do not overlap with the putative DNA-binding loops L1 and L2 (amino acid residues 235–240 and 271–286) that face towards the center of the ring or the filament structure. This fact is consistent with the results that $RAD54B_{26-225}$ interacted with the DMC1 bound to either ssDNA or dsDNA. Interestingly, the corresponding RAD54B-interacting regions of RadA are located near the monomer–monomer interface, and contain amino acid residues that directly interact with ATP (Figure 6). Thus, the N-terminal region of RAD54B may affect the quaternary structure of DMC1 through these interactions, and may be critical for regulating the function of DMC1. Given that RAD54B stimulates the DMC1-mediated DNA strand exchange, one possibility is that the binding of RAD54B to DMC1 may trigger the conversion of the DMC1 structure from the octameric ring form to the active helical filament form. Another possibility is that the binding of RAD54B to DMC1 may promote the turnover of DMC1 from the DNA strand-exchange product, leading to the release of DMC1. Although these observations suggested that the interaction between RAD54B and DMC1 is functionally important, meiosis in the *RAD54B* knockout mouse seems to be unaffected (29). This may be due to the presence of an unidentified RAD54 paralog that functions in meiosis. Alternatively, RAD54B may have a relatively minor role in meiosis, and may function with DMC1 only under certain circumstances. Further *in vivo* and *in vitro* analyses are required to elucidate the role of RAD54B in meiosis.

In conclusion, the present study demonstrated that the N-terminal region of RAD54B is multifunctional. We found several novel biochemical properties of the N-terminal region of RAD54B that were not previously shown for the corresponding region in RAD54. These activities may be essential for the specialized role of RAD54B in homologous recombination. More studies are required to understand the broad functional spectra of RAD54B in homologous recombination, including those that are unique to RAD54B and those that are commonly shared among RAD54 paralogs.

ACKNOWLEDGEMENTS

We thank Dr Takashi Kinebuchi (Olympus) for technical assistance.

FUNDING

Targeted Proteins Research Program (TPRP); RIKEN Structural Genomics/Proteomics Initiative (RSGI) of the National Project on Protein Structural and Functional Analyses, MEXT. The Open Access publication charges for this manuscript were waived by Oxford University Press.

Conflict of interest statement. None declared.

REFERENCES

1. Cox,M.M., Goodman,M.F., Kreuzer,K.N., Sherratt,D.J., Sandler,S.J. and Marians,K.J. (2000) The importance of repairing stalled replication forks. *Nature*, **404**, 37–41.
2. Ward,J.F. (1994) The complexity of DNA damage: relevance to biological consequences. *Int. J. Radiat. Biol.*, **66**, 427–432.
3. Caldecott,K.W. (2001) Mammalian DNA single-strand break repair: an X-ra(y)ted affair. *Bioessays*, **23**, 447–455.
4. Kleckner,N. (1996) Meiosis: how could it work? *Proc. Natl Acad. Sci. USA*, **93**, 8167–8174.
5. Roeder,G.S. (1997) Meiotic chromosomes: it takes two tango. *Genes Dev.*, **11**, 2600–2621.

6. Keeney,S., Gitoux,C.N. and Kleckner,N. (1997) Meiosis-specific DNA double-strand breaks are catalyzed by Spo11, a member of a widely conserved protein family. *Cell*, **88**, 375–384.
7. Symington,L.S. (2002) Role of RAD52 epistasis group genes in homologous recombination and double-strand break repair. *Microbiol. Mol. Biol. Rev.*, **66**, 630–670.
8. Krogh,B.O. and Symington,L.S. (2004) Recombination protein in yeast. *Annu. Rev. Genet.*, **38**, 233–271.
9. Eisen,J.A., Sweder,K.S. and Hanawalt,P.C. (1995) Evolution of the SNF2 family of proteins: subfamilies with distinct sequences and functions. *Nucleic Acids Res.*, **23**, 2715–2723.
10. Swagemakers,S.M., Essers,J., de Wit,J., Hoeijmakers,J. H. and Kanaar,R. (1998) The human RAD54 recombinational DNA repair protein is a double-stranded DNA-dependent ATPase. *J. Biol. Chem.*, **273**, 28292–28297.
11. Alexiadis,V. and Kadonaga,J.T. (2002) Strand pairing by Rad54 and Rad51 is enhanced by chromatin. *Genes Dev.*, **16**, 2767–2771.
12. Alexeev,A., Mazin,A. and Kowalczykowski,S.C. (2003) Rad54 protein possesses chromatin-remodeling activity stimulated by the Rad51-ssDNA nucleoprotein filament. *Nat. Struct. Biol.*, **10**, 182–186.
13. Jaskelioff,M., Van Komen,S., Krebs,J.E., Sung,P. and Peterson,C.L. (2003) Rad54p is a chromatin remodeling enzyme required for heteroduplex DNA joint formation with chromatin. *J. Biol. Chem.*, **278**, 9212–9218.
14. Wolner,B. and Peterson,C.L. (2005) ATP-dependent and ATP-independent roles for the Rad54 chromatin remodeling enzyme during recombinational repair of a DNA double strand break. *J. Biol. Chem.*, **280**, 10855–10860.
15. Alexiadis,V., Lusser,A. and Kadonaga,J.T. (2004) A conserved N-terminal motif in Rad54 is important for chromatin remodeling and homologous strand pairing. *J. Biol. Chem.*, **279**, 27824–27829.
16. Tan,T.L.R., Kanaar,R. and Wyman,C. (2003) Rad54, a Jack of all trades in homologous recombination. *DNA Repair*, **2**, 787–794.
17. Heyer,W.D., Li,X., Rolfsmeier,M. and Zhang,X.P. (2006) Rad54: the Swiss Army knife of homologous recombination? *Nucleic Acids Res.*, **34**, 4115–4125.
18. Jiang,H., Xie,Y., Houston,P., Stemke-Hale,K., Mortensen,U.H., Rothstein,R. and Kodadek,T. (1996) Direct association between the yeast Rad51 and Rad54 recombination proteins. *J. Biol. Chem.*, **271**, 33181–33186.
19. Golub,E.I., Kovalenko,O.V., Gupta,R.C., Ward,D.C. and Radding,C.M. (1997) Interaction of human recombination proteins Rad51 and Rad54. *Nucleic Acids Res.*, **25**, 4106–4110.
20. Wolner,B., van Komen,S., Sung,P. and Peterson,C.L. (2003) Recruitment of the recombinational repair machinery to a DNA double-strand break in yeast. *Mol. Cell*, **12**, 221–232.
21. Mazin,A.V., Alexeev,A.A. and Kowalczykowski,S.C. (2003) A novel function of Rad54 protein. Stabilization of the Rad51 nucleoprotein filament. *J. Biol. Chem.*, **278**, 14029–14036.
22. Petukhova,G., Stratton,S. and Sung,P. (1998) Catalysis of homologous DNA pairing by yeast Rad51 and Rad54 proteins. *Nature*, **393**, 91–94.
23. Sigurdsson,S., Van Komen,S., Petukhova,G. and Sung,P. (2002) Homologous DNA pairing by human recombination factors Rad51 and Rad54. *J. Biol. Chem.*, **277**, 42790–42794.
24. Solinger,J.A., Lutz,G., Sugiyama,T., Kowalczykowski,S.C. and Heyer,W.D. (2001) Rad54 protein stimulates heteroduplex DNA formation in the synaptic phase of DNA strand exchange via specific interactions with the presynaptic Rad51 nucleoprotein filament. *J. Mol. Biol.*, **307**, 1207–1221.
25. Bugreev,D.V., Mazina,O.M. and Mazin,A.V. (2006) Rad54 protein promotes branch migration of Holliday junction. *Nature*, **442**, 590–593.
26. Solinger,J.A., Kiianitsa,K. and Heyer,W.D. (2002) Rad54, a Swi2/Snf2-like recombinational repair protein, disassembles Rad51:dsDNA filaments. *Mol. Cell*, **10**, 1175–1188.
27. Hiramoto,T., Nakanishi,T., Sumiyoshi,T., Fukuda,T., Matsuura,S., Tauchi,H., Komatsu,K., Shibasaki,Y., Inui,H., Watatani,M. *et al.* (1999) Mutation of a novel human RAD54 homologue, RAD54B, sin primary cancer. *Oncogene*, **18**, 3422–3426.
28. Tanaka,K., Kagawa,W., Kinebuchi,T., Kurumizaka,H. and Miyagawa,K. (2002) Human Rad54B is a double-stranded DNA-dependent ATPase and has biochemical properties different from its structural homolog in yeast, Tid1/Rdh54. *Nucleic Acids Res.*, **30**, 1346–1353.
29. Wesoly,J., Agarwal,S., Sigurdsson,S., Bussen,W., Van Komen,S., Qin,J., Van Steeg,H., Van Benthem,J., Wassenaar,E., Baarends,W.M. *et al.* (2006) Differential contributions of mammalian Rad54 paralogs to recombination, DNA damage repair, and meiosis. *Mol. Cell Biol.*, **26**, 976–989.
30. Sarai,N., Kagawa,W., Kinebuchi,T., Kagawa,A., Tanaka,K., Miyagawa,K., Ikawa,S., Shibata,T., Kurumizaka,H. and Yokoyama,S. (2006) Stimulation of Dmc1-mediated DNA strand exchange by the human Rad54B protein. *Nucleic Acids Res.*, **34**, 4429–4437.
31. Sehorn,M.G., Sigurdsson,S., Bussen,W., Unger,V.M. and Sung,P. (2004) Human meiotic recombinase Dmc1 promotes ATP-dependent homologous DNA strand exchange. *Nature*, **429**, 433–437.
32. Zhang,Z., Fan,H.Y., Goldman,J.A. and Kingston,R.E. (2007) Homology-driven chromatin remodeling by human RAD54. *Nat. Struct. Mol. Biol.*, **14**, 397–405.
33. Kagawa,W., Kurumizaka,H., Ikawa,S., Yokoyama,S. and Shibata,T. (2001) Homologous pairing promoted by the human Rad52 protein. *J. Biol. Chem.*, **276**, 35201–35208.
34. Kinebuchi,T., Kagawa,W., Enomoto,R., Tanaka,K., Miyagawa,K., Shibata,T., Kurumizaka,H. and Yokoyama,S. (2004) Structural basis for octameric ring formation and DNA interaction of the human homologous-pairing protein Dmc1. *Mol. Cell*, **14**, 363–374.
35. Parsons,C.A., Kemper,B. and West,S.C. (1990) Interaction of a four-way junction in DNA with T4 endonuclease VII. *J. Biol. Chem.*, **265**, 9285–9289.
36. Whitby,M.C. and Dixon,J. (1998) Targeting Holliday junctions by the RecG branch migration protein of Escherichia coli. *J. Biol. Chem.*, **273**, 35063–35073.
37. Osman,F., Dixon,J., Doe,C.L. and Whitby,M.C. (2003) Generating crossovers by resolution of nicked Holliday junctions: a role for Mus81-Eme1 in meiosis. *Mol. Cell*, **12**, 761–774.
38. Miyagawa,K., Tsuruga,T., Kinomura,A., Usui,K., Katsura,M., Tashiro,S., Mishima,H. and Tanaka,K. (2002) A role for RAD54B in homologous recombination in human cells. *EMBO J.*, **21**, 175–180.
39. Tanaka,K., Hiramoto,T., Fukuda,T. and Miyagawa,K. (2000) A novel human rad54 homologue, Rad54B, associates with Rad51. *J. Biol. Chem.*, **275**, 26316–26321.
40. Thoma,N.H., Czyzewski,B.K., Alexeev,A.A., Mazin,A.V., Kowalczykowski,S.C. and Pavletich,N.P. (2005) Structure of the SWI2/SNF2 chromatin-remodeling domain of eukaryotic Rad54. *Nat. Struct. Mol. Biol.*, **12**, 350–356.
41. Petukhova,G., Van Komen,S., Vergano,S., Klein,H. and Sung,P. (1999) Yeast Rad54 promotes Rad51-dependent homologous DNA pairing via ATP hydrolysis-driven change in DNA double helix conformation. *J. Biol. Chem.*, **274**, 29453–29462.
42. Mazina,O.M., Rossi,M.J., Thoma,N.H. and Mazin,A.V. (2007) Interactions of human Rad54 protein with branched DNA molecules. *J. Biol. Chem.*, **282**, 21068–21080.
43. Wu,Y., Qian,X., He,Y., Moya,I.A. and Luo,Y. (2005) Crystal structure of an ATPase-active form of Rad51 homolog from Methanococcus voltae. *J. Biol. Chem.*, **280**, 722–728.
44. DeLano,W.L. (2002) *The PyMOL Molecular Graphics System*. DeLano Scientific, San Carlos, CA, USA.

J. Radiat. Res., 49, 93–103 (2008) Review

Current Topics in DNA Double-Strand Break Repair

Junya KOBAYASHI[1], Kuniyoshi IWABUCHI[2], Kiyoshi MIYAGAWA[3], Eiichiro SONODA[4], Keiji SUZUKI[5], Minoru TAKATA[6] and Hiroshi TAUCHI[7]*

DNA repair/Homologous recombination/Nuclear foci/Non-homologous end joining.

DNA double strand break (DSB) is one of the most critical types of damage which is induced by ionizing radiation. In this review, we summarize current progress in investigations on the function of DSB repair-related proteins. We focused on recent findings in the analysis of the function of proteins such as 53BP1, histone H2AX, Mus81-Eme1, Fanc complex, and UBC13, which are found to be related to homologous recombination repair or to non-homologous end joining. In addition to the function of these proteins in DSB repair, the biological function of nuclear foci formation following DSB induction is discussed.

1. INTRODUCTION: AT the broken DNA ends

Ionizing radiation (IR) induces a variety of DNA lesions, including single- and double-strand breaks, DNA-protein cross-links, and various base damages. A DNA double-strand break (DSB) is one of the most serious threats to cells because it can result in loss or rearrangement of genetic information, leading to cell death or carcinogenesis. There are at least two repair pathways which can repair DSBs: (1) non-homologous end-joining (NHEJ)- and/or micro-homology-mediated recombination, and (2) homologous recombination (HR)-mediated repair.[1)] These damage responding repair pathways are thought to be regulated by several major steps. First, a sensor protein (probably, ATM or Rad50/Mre11/NBS1 complex) recognizes damage induction by radiation. Second, mediator proteins receive a structural modification by the sensor protein(s), and this modification is converted to a compatible form for signal amplification by transducer proteins. These transducers amplify the signal, and finally, effector proteins accomplish enzymatic reactions of DNA end processing, rejoining, or cell cycle regulation. Figure 1 shows a brief overview of relationship among radiation-DSB responding factors. When DSBs are generated, ATM protein kinase is activated and relocates through an interaction with Rad50/Mre11/NBS1 complex.[2)] Then ATM phosphorylates histone H2AX and many other substrate proteins including Artemis, MDC1, NBS1, p53, Chk2, and DNA-PKcs kinase. ATM-phosphorylated proteins activate cell cycle checkpoints, NHEJ repair pathway, and HR repair-related pathways. Hence, ATM kinase, whose mutation causes a genetic disorder, ataxia-telangiectasia (AT), at the broken DNA ends is an central regulator of the DSB responding pathway. In addition to signal transduction, many proteins involved in damage response, including activated ATM itself, form nuclear foci (see chapters 3, 7, and Fig. 7). Recently, it has been found that proteins involved in HR pathway are often ubiquitinated and this seems to be essential for HR repair (chapter 6).

In this review, we summarize current topics in DNA repair with a focus on the function of proteins related to HR repair (chapters 4, 5, and 6), a novel NHEJ pathway that is mediated by 53BP1 (chapter 2), and the biological function of nuclear foci formation of damage sensor or mediator proteins (chapters 3 and 7).

2. 53BP1-dependent repair pathway for X-ray-induced DNA damage

DSBs activate signaling responses, termed cell-cycle checkpoints, which monitor DNA damage and transduce signals to coordinate repair and cell cycle progression.[3)] One

*Corresponding author: Phone: +81-29-228-8383,
Fax: +81-29-228-8403,
E-mail: htauchi@mx.ibaraki.ac.jp

[1]Department of Genome Repair Dynamics, Radiation Biology Center, Kyoto University, Yoshida-Konoe, Sakyo-ku, Kyoto 606-8501 Japan; [2]Department of Biochemistry, Kanazawa Medical University, Daigaku 1-1, Uchinada, Kahoku-gun, Ishikawa 920-0293, Japan; [3]Section of Radiation Biology, Graduate School of Medicine, The University of Tokyo, 7-3-1 Hongo, Bunkyo-ku, Tokyo 113-0033, Japan; [4]Department of Radiation Genetics, Faculty of Medicine, Kyoto University, Yoshida Konoe, Sakyo-ku, Kyoto 606-8501 Japan; [5]Graduate school of Biomedical Sciences, Nagasaki University, 1-12-4 Sakamoto, Nagasaki 852-8523, Japan; [6]Department of Late Effects Studies, Radiation Biology Center, Kyoto University, Yoshida-Konoe, Sakyo-ku, Kyoto 606-8501 Japan; [7]Department of Environmental Sciences, Faculty of Science, Ibaraki University, Bunkyo 2-1-1, Mito, Ibaraki 310-8512 Japan.
doi:10.1269/jrr.07130

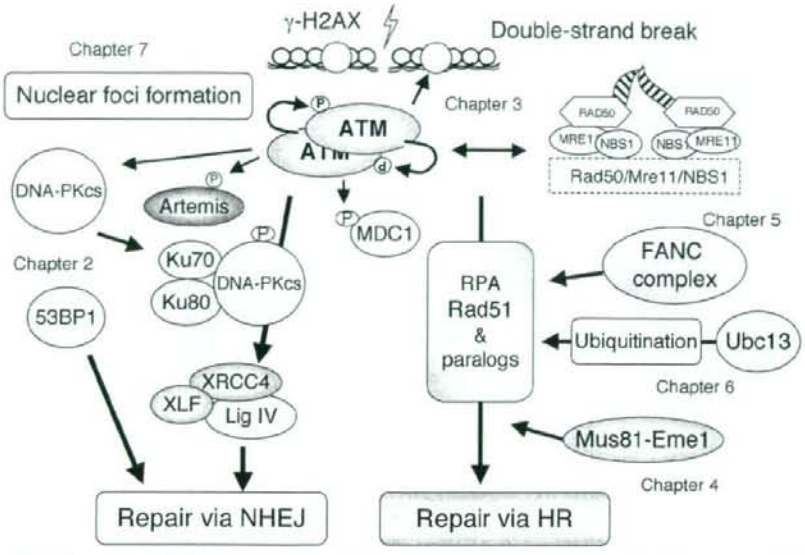

Fig. 1. Proteins related to DNA double strand break repair. Relevant chapter numbers in this review are indicated.

of the key players of cell-cycle checkpoints is the tumor suppressor protein p53. p53 is activated and posttranscriptionally modified in response to DNA damage. These modifications include phosphorylation by ataxia telangiectasia mutated (ATM), a central signaling kinase in the response to DNA damage.[4] p53 transcriptionally activates genes involved in cell cycle control, DNA repair and apoptosis, and participates in the maintenance of the genome integrity after DNA damage.[3]

Using the yeast two-hybrid system, 53BP1 was identified as a protein that binds to wild type p53.[5,6] Human 53BP1 consists of 1972 amino acid residues, the C-terminus of which contains tandem BRCA1 C-terminus (BRCT) motifs. 53BP1 binds to the DNA-binding domain of p53 through 53BP1's BRCT motifs.[7,8] BRCT domain is found in a large number of proteins involved in the cellular responses to DNA damage, suggesting 53BP1's roles in these aspects. Consistently, 53BP1 rapidly forms discrete nuclear foci in response to γ-radiation.[9,10] These foci colocalize with phosphorylated H2AX (γ-H2AX), a marker of DNA DSBs, indicating that 53BP1 relocalizes to sites of DNA DSBs in response to γ-radiation. The minimal domain for focus formation consists of tandem Tudor motifs,[11] which have been reported to associate with various methylated lysine residues in histone H3 and H4. These include lysines K79 in histone H3 and K20 in histone H4.[12,13] Although methylation of histone H3 K79 is unaltered in response to DNA damage, K79 lies in the nucleosome core, and is inaccessible under normal conditions. Because of this, 53BP1 is proposed to sense changes in higher-order chromatin structure.[12]

53BP1 becomes hyperphosphorylated in response to γ-radiation.[10,14,15] ATM-deficient cells show no 53BP1 hyperphosphorylation, and inhibition of phosphatidylinositol 3-kinase family by wortmannin strongly inhibited γ-radiation-induced hyperphosphorylation. In addition, 53BP1 is readily phosphorylated by ATM *in vitro*. These results suggest that 53BP1 is an ATM substrate that is involved in cellular responses to DSBs. However, there is some evidence that 53BP1 have a role in DNA damage signaling upstream of ATM. Analysis of mammalian cell lines depleted in 53BP1 expression through small interfering RNA revealed that 53BP1 is required for accumulation of p53, G2-M checkpoint, intra-S-phase checkpoint, and optimal phosphorylation of at least a subset of ATM substrates such as Chk2, BRCA1 and Smc1 in response to radiation-induced DNA damages.[16,17,18] These results indicate that 53BP1 is a central mediator of the DNA damage checkpoints.[16]

The Tudor motifs also stimulate end-joining by DSB repair proteins DNA ligase IV/Xrcc4, but not by T4 DNA ligase *in vitro*.[19] This suggests that 53BP1 has the potential to participate directly in the repair of DNA DSBs. DSBs are repaired by two major pathways: HR and NHEJ.[20,21] HR primarily uses the undamaged sister chromatid as a DNA template allowing for accurate repair of the lesions, and functions in late S-G2 phase. NHEJ is an error-prone joining of DNA ends with the use of little or no sequence homology, and plays a major role in the repair of IR-induced DSBs, especially during the G1 phase of the cell cycle when sister

chromatids are not available.[22] Riballo and their colleagues proposed a model for the repair of IR-induced DSBs during the G1 phase in mammalian cells, in which the majority of DSBs are rejoined by the "core NHEJ", but repair of a subfraction of DSBs requires Artemis, an endonuclease required for processing the hairpin intermediate generated during V(D)J recombination.[23] The "core NHEJ" is composed of Lig IV/Xrcc4, Ku70/Ku80, and DNA-PKcs. Artemis is a downstream component of ATM-dependent signaling in DSB repair, and the ATM/Artemis-dependent repair pathway also requires proteins locating to sites of DSBs, including 53BP1.[23] However, in chicken DT40 cells, 53BP1 seems to contribute to survival of cells irradiated with IR during the G1 without Ku70 or Artemis. We established 53BP1-deficient chicken DT40 cells.[24] 53BP1-deficient cells show increased sensitivity to X-rays during G1 phase. Although intra-S and G2/M checkpoints are intact, a frequency of isochromatid-type chromosomal aberrations is elevated after irradiation in 53BP1-deficient cells. Furthermore, disappearance of X-ray-induced γ-H2AX foci is prolonged in 53BP1-deficient cells. Thus, the elevated X-ray sensitivity in G1 phase cells is attributable to repair defect for IR-induced DNA-damage. Epistasis analysis revealed that 53BP1 is non-epistatic with Ku70 and Artemis, but epistatic with DNA ligase IV. Strikingly, disruption of the *53BP1* gene together with inhibition of phosphatidylinositol 3-kinase family by wortmannin completely abolishes colony formation by cells irradiated during G1 phase. These results demonstrate that there is a 53BP1-dependent repair pathway which is distinct from the Ku70-dependent and Artemis-dependent NHEJ pathways (Fig. 2).

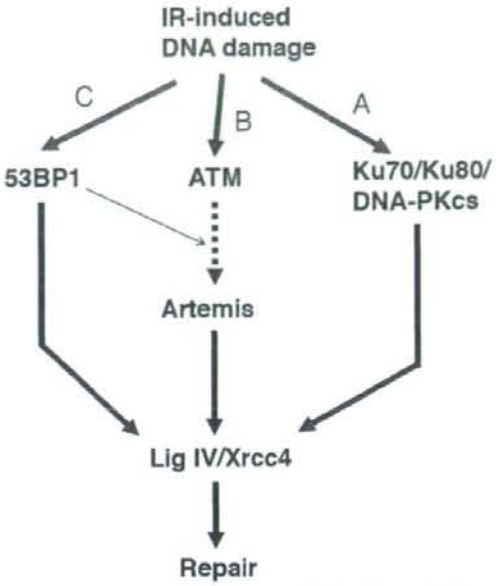

Fig. 2. Model of the repair pathways for IR-induced DNA damage in G1 phase cells. A, B and C represent the core NHEJ, ATM/Artemis-dependent and 53BP1-dependent pathways, respectively. The dotted arrow represents the minor pathway in DT40 cells. The thin arrow represents a possible interaction resulting from the scaffold function of 53BP1.

The 53BP1-dependent pathway made a larger contribution to cell survival in G1 than in early S phase,[24] suggesting that the 53BP1-dependent pathway is regulated at the G1 to S phase transition by mechanisms distinct from the other two pathways. It has been shown that 53BP1-deficient mice have intact V(D)J recombination but impaired class switch recombination.[25,26] It is unclear whether the 53BP1-dependent repair pathway is involved in class switch recombination. However, if, as proposed,[27] class switch recombination occurs in the G1 phase of the cell cycle, it is possible that, in vertebrates, class switch recombination is the main stage at which 53BP1 participates in DNA damage repair.

3. Role of NBS1 and histone H2AX in DNA double-strand break repair

Nijmegen breakage syndrome (NBS) is a radiation-hypersensitive genetic disorder. NBS and AT show the similar cellular phenotypes such as radiation-hypersensitivity, chromosomal instability and radiation-resistant DNA synthesis.[28] So far, it has been clarified that the responsible gene product of NBS, NBS1, interacts with ATM (the responsible gene product of AT syndrome) and this interaction is indispensable for the recruitment of ATM to DSB sites and activation of ATM kinase.[29] Hence, the functional interaction between NBS1 and ATM is important for the regulation of cell cycle checkpoints. Previously, we reported that NBS1 formed a complex with MRE11 nuclease and RAD50 and worked for HR repair in DT-40 chicken cells.[30] Moreover, NBS1 forms the complex with γ-H2AX in response to DSB damage, and this interaction is essential to the recruitment of NBS1 to DSB sites.[31] These facts suggest that the NBS1 complex may function for DSB repair together with ATM and γ-H2AX in human cells. NBS1 has BRCT and FHA domains in the N-terminus, ATM-phosphorylating sites in the central region, and hMRE11 and ATM-binding sites in the C-terminus (Fig. 3). Therefore, we investigated the role of these domains for HR repair using a DR-GFP assay.[32]

The mutation of NBS1 in BRCT, FHA or MRE11-binding domain decreased HR activity, and NBS cells expressing these mutated NBS1 cannot form DSB-induced MRE11 foci. These results indicate that the recruitment of MRE11 to the DSB site by NBS1 is important for HR activity. On the other hand, the mutation in ATM-phosphorylating or ATM-binding sites did not influence the HR activity. Moreover, AT cells showed an HR activity at a similar level as

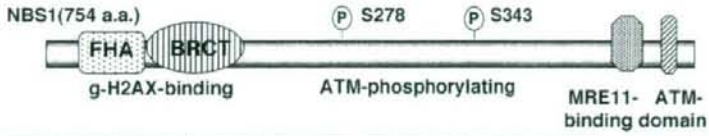

mutated site	FHA	BRCT	ATM-phosphorylating	MRE11-binding	ATM-binding
HR activity	-	-	+	-	+
NBS1 foci	-	-	+	+	+
MRE11 foci	-	-	+	-	+

Fig. 3. Characteristic domains of NBS1. The domains (FHA, BRCT, MRE11-binding), which are essential for DSB-induced foci formation of MRE11, are indispensable for HR activity. The table summarizes the relationship between the site of NBS1 mutation and DNA damage response (HR activity, NBS1 foci formation, and MRE11 foci formation). (+): a little or no effect. (−): abrogate the listed function.

ATM-complemented cells, suggesting that ATM might be dispensable for HR repair. As γ-H2AX interacts with NBS1 through the FHA/BRCT domain, we also examined the role of H2AX in HR repair. H2AX-knockout ES cells showed a decrease in HR activity, and the mutation into the acetylated or sumoylated site of H2AX influenced the DSB-induced foci formation and HR activity. Sumoylation of H2AX was confirmed by an *in vitro E. coli* sumoylation system.[33] Furthernore, the repression of acetylation at common sites between H2A and H2AX by a specific inhibitor also decreased IR-induced foci formation and HR activity. These results suggest that the modification of H2AX is related to the recruitment of DSB-related proteins and to HR repair. Taken together, both NBS1 and H2AX could function in HR repair, although ATM, which functionally and physically interacts with NBS1, is dispensable for HR.

4. The role of the Mus81-Eme1 endonuclease in maintenance of genome integrity

The heterodimeric Mus81-Eme1 structure-specific endonuclease plays a role in perturbed replication fork processing and DNA repair by HR. The complex preferentially cleaves nicked Holliday junctions, aberrant replication fork structures, D-loops, and 3'-flap structures, suggesting its roles both upstream and downstream of HR.[34] Dysfunction of Mus81-Eme1 leads to hypersensitivity to a wide range of DNA-damaging agents. In yeast, mus81 mutants are hypersensitive to ultraviolet light, methylmethane sulfonate, camptothecin, and hydroxyurea, suggesting a role for the endonuclease in the rescue of stalled and collapsed replication forks.[35] In contrast, murine and human Mus81 and Eme1 mutant cells are hypersensitive to mitomycin C and cisplatin but not to camptothecin.[36,37] In addition, Mus81-Eme1 has been proposed to play a role in processing spontaneous DNA damage[38]. In this chapter, evidence that the complex is involved in the maintenance of genome integrity is assessed.

An increase in chromosome aberrations represented by breaks, triradials, dicentrics, and fusions is observed in Mus81 and Eme1-deficient mammalian cells.[38,39] Furthermore, the frequency of aneuploidy is increased in these cells. Remarkably, haploinsufficiency of Mus81 or Eme1 also leads to these aberrations, suggesting that the proper biallelic expression of Mus81 and Eme1 is required for the maintenance of chromosome integrity in mammalian cells. Because these aberrations are observed in the absence of exogenous DNA damage, Mus81-Eme1 plays a role in processing spontaneous DNA lesions.

$Mus81^{-/-}$ murine cells accumulate in G2. Phosphorylation of Chk1 is elevated in these cells, indicating that the Chk1-mediated checkpoint is activated in response to spontaneous DNA damage.[37] We examined the mechanisms underlying checkpoint activation using synchronized human HCT116 cells.[38] Both damage-induced Chk1 and Chk2 phosphorylation was increased in Mus81 or Eme1 mutant cells during the S phase. Silencing of ATM reduced the frequency of cells with damage-induced Chk1 or Chk2 phosphorylation, whereas silencing of ATR did not affect the frequency. In addition, phosphorylation of Chk2 was increased in these cells in G2, which was reduced by silencing of ATM. These observations suggest that spontaneous DNA damage generated by Mus81-Eme1 dysfunction activates both the intra-S-phase and G2 checkpoints (Fig. 4).

The p53-mediated checkpoint activation is not observed in $Mus81^{-/-}$ cells in the absence of exogenous DNA damage.[38] However, increased activation of p53 is observed in $Mus81^{-/-}$ cells compared with wild-type cells following mitomycin C treatment.[40] This observation suggests that the p53-dependent checkpoint is activated in response to interstrand cross-linking-induced DNA damage in the absence of Mus81.

Both $Mus81^{+/-}$ and $Mus81^{-/-}$ mice exhibited a profound predisposition to lymphomas and other solid tumors.[39]

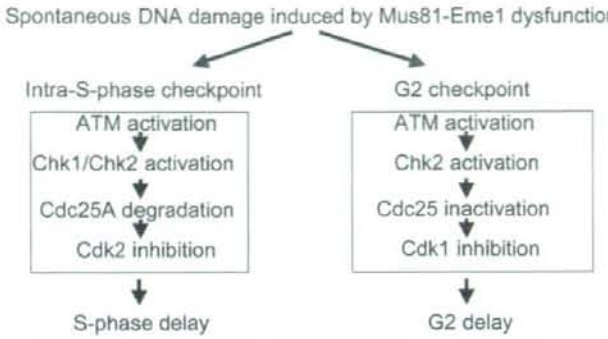

Fig. 4. Checkpoint activation in response to spontaneous DNA damage in HCT116 cells with Mus81 or Eme1 dysfunction.

However, no increased susceptibility of tumor has been observed in another mouse model.[37] It is therefore possible that Mus81-Eme1 dysfunction does not directly lead to tumorigenesis but rather contributes to chromosome instability. Importantly, a recent study has indicated that loss of one allele of Mus81 increases the predisposition of $p53^{-/-}$ mice to sarcoma.[40] This observation suggests that Mus81 may play a role in suppressing sarcoma formation in collaboration with p53.

Thus, accumulating evidence suggests that cellular checkpoints are activated in response to both spontaneous and exogenous DNA damage in cells with Mus81-Eme1 dysfunction. Mus81-Eme1 is therefore likely to play a role in the maintenance of genome integrity in collaboration with multiple checkpoint pathways.

5. FA pathway and homologous recombination repair

Fanconi anemia (FA) is a rare hereditary disorder characterized by progressive bone marrow failure, compromised genome stability, and increased incidence of cancer (reviewed in Wang 2007.[41] FA is caused by genetic defects in altogether 13 genes but this number may further increase in the future. These include genes encoding components of the FA core complex (FancA/B/C/E/F/G/L/M), a key factor FancD2, breast cancer susceptibility protein BRCA2/FancD1, BRCA2's partner PALB2/FancN, BRIP1/FancJ helicase, and just recently discovered FancI. In addition, there are a few gene products that associate with the FA core complex (i.e. FAAP100 and FAAP24 proteins) but without known FA patients lacking these factors.[41]

It has been well known that cells from FA patients display hypersensitivity to DNA crosslinks,[42] and in this regard they seems to resemble cells deficient in HR proteins such as Rad51 paralogs.[43,44] Moreover, they are often mildly sensitive to ionizing irradiation as well. These data may support an idea that basic defects in FA patients could be related to DNA DSB repair. However, until recently, the role played by FA proteins is largely unknown, except for the case of BRCA2, which regulates the central HR protein Rad51.[45] In the DNA damage response, FancD2 and FancI proteins (they form D2-I complex) are targeted to chromatin and forms nuclear foci following their monoubiquitination, a process likely catalyzed by the FA core complex.[41] These foci colocalize at least partially with Rad51 as well as BRCA1.[46] The monoubiquitination is critical for regulating nuclear dynamics of FancD2 (unpublished) as well as tolerance to cisplatin treatment.[47,48] BRCA2/FancD1, PALB2/FANCN, and BRIP1 helicase are not required for FancD2/FancI monoubiquitination, but they should act downstream of, or in parallel to, the core complex-FancD2/FancI pathway.[41]

We planed to examine function of the FA pathway by making knockout cell lines lacking FA proteins in chicken B cell line DT40.[49] The rationale to choose this system is that there are a number of HR assays that could be performed in DT40 cells, and other genetic models such as yeast *S. cerevisiae* do not have a set of FA genes.[41] Our DT40 FA mutant cell lines display similar basic phenotypes. They grow slower than wild type cells, and are hypersensitive to DNA crosslink inducer cisplatin, while radiation sensitivity is quite mild. We first tried to examine whether these mutant cells show defects in HR repair of chromosomal DSB induced by restriction enzyme I-SceI. In this assay, cells that have undergone HR repair form neo-resistant colonies, and the number of the colonies indicates DSB repair activity mediated by HR. We found that *FANCD2*- or *FANCG*-deficient cells are indeed defective in this HR assay.[50,51] Our report was the first to show that the FA pathway is required for normal HR repair. Then we looked at the repaired chromosomal site in *fancd2* cells by Southern blotting, and found that HR repair in this system was compromised not only quantitatively but also qualitatively.[51] The mode of the HR repair was altered such that fraction of long tract gene conversion (LTGC) was decreased from 15% to

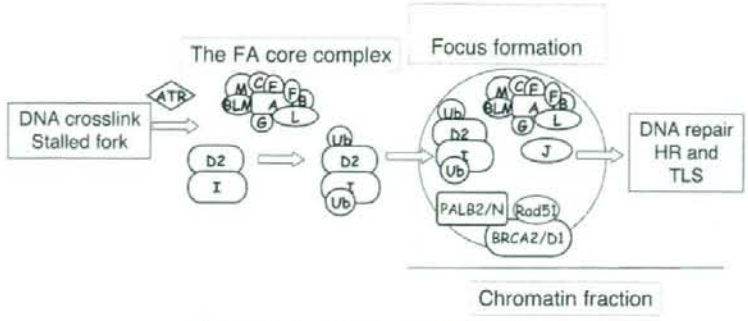

Fig. 5. A simplified view of the FA pathway.

2.7%. Furthermore, ~5% of cells undergo aberrant repair that apparently started with HR but ended by ligation due to non-homologous end joining.[51]

The utility of the DT40 system in HR research is highlighted by the phenomenon "immunoglobulin gene conversion (Ig GCV)". Chicken B lymphocytes diversify its Ig variable gene by GCV mechanism, which depends on Ig transcription, AID expression, and a set of HR factors.[52] DT40 is originated in retrovirally-induced lymphoma in the Bursa of Fabricius, and still continues GCV in *in vitro* culture condition.[53] We found Ig GCV occurs at significantly reduced rate in *fancd2* cells, which is consistent with a role of the FA pathway in HR.[51]

HR repair is proficient mainly during late S to G2 phases in the cell cycle,[54] perhaps because of availability of the template (sister chromatid) and DSB end processing regulated by CDK[55] as well as CtIP protein.[56,57] Therefore we expected that FA protein deficiency should affect DSB repair in those cell cycle phases. Indeed, we found that synchronized *fancd2*-deficient cells display higher radiation sensitivity in late S to G2 phase compared to G1 to early S phases.[51] Kinetics analysis of IR-induced chromosome aberration also supported this notion. Then we looked at IR sensitivity in *ku70/fancg* double knockout cells. In the absence of Ku70 protein, a critical NHEJ factor, DT40 cells are more tolerant to IR than wild type in higher dose range (4–12 Gy),[54] suggesting that presence of Ku may hampers access of HR factors to the broken ends.[58] The double knockout cells are slightly but significantly more IR sensitive than *ku70* single knockout cells (unpublished data), consistent with the role of the FA pathway in HR but not in NHEJ.

We have also analyzed relationship between the classical FA pathway (the core complex-FancD2-FancI pathway) and FancD1/BRCA2.[59] BRCA2 is essential for IR- or MMC-induced Rad51 foci formation but not for FancD2 foci formation, suggesting that the former is not a prerequisite for the latter. Likewise, FancD2 foci formation is not required for Rad51 foci formation. Consistently, DNA damage-induced chromatin loading of Rad51 is normal in cells deficient in FA proteins, raising a possibility that the FA pathway and BRCA2-Rad51 pathway are, at least in their activation phase, independent with each other and in a parallel relationship.[59]

In conclusion, our data clearly demonstrated that the FA pathway participates HR repair (more extensively reviewed in Takata et al. 2006, 2007).[49,60] Interestingly, *BRCA2/FANCC* double knockout cells show similar levels of IR sensitivity with BRCA2 mutant.[59] Taken into account with Rad51 focus and chromatin loading data, this may suggest the FA pathway acts downstream of Rad51. However, further work is needed to draw definite conclusion regarding the function of the FA pathway.

6. UBC13, a ubiqutin E2 conjugating enzyme, plays critical roles in homologous recombination-mediated double strand break repair

Ubiquitylation is involved in DNA repair including nucleotide excision repair, crosslink repair, and postreplication repair (PRR). Rad6/Rad18, a ubiquitin E2/E3 enzyme complex, monoubiquitinates lysine 164 of PCNA, thereby facilitates the loading of translesion polymerases including Polη at blocked forks to resume replication.[61,62] Another E2 enzyme, Ubc13 poly-ubiquitinates PCNA through lysine 63 of ubiquitine (K63) to regulate PRR in yeast. K63 poly-ubiquitination does not appear to involve recognition by the proteasome,[63,64] and its role in damage response has been unclear.

Zhao in Takeda's laboratory recently reported that vertebrate Ubc13 plays a critical role in HR-mediated DSB repair as well as PRR.[65] UBC13$^{-/-}$ DT40 cells show hypersensitivity to a wide range of DNA damaging agents including UV, X-ray, cross-linkers and camptothecin, and exhibit impaired extension of nascent strand over damaged templates, indicating a conserved role for Ubc13 in PRR in eukaryotic species.

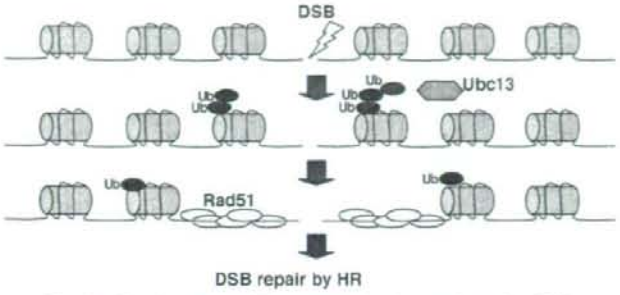

Fig. 6. Ubc13 promotes HR by ubiquitinating proteins at the DSB.

In yeast, Rad18 and Ubc13 are involved in PRR but not HR. Surprisingly, Ubc13$^{-/-}$ DT40 and Ubc13 knockdown human cells show a severe defect in HR as evidenced by a decrease in the frequency of gene targeting and the defective DSB repair of artificial HR substrates. To understand the cause of defective HR, we measured ionizing radiation-induced focus formation. The loss of Ubc13 reduces the focus formation of RPA, a single-strand (ss) binding protein, Brca1, and Rad51 but not that of γ-H2AX or autophosphorylated ATM (ATM$^{P[981]}$). These results suggest that Ubc13 is required for the formation of a single-stranded overhang that is essential for the assembly of Rad51 at DSB ends. To explore a substrate for Ubc13 mediated ubiquitylation, we monitored IR-induced FK2 focus formation, which represents intensive conjugated ubiquitylation at the site of DSB. *UBC13*$^{-/-}$ DT40 cells show virtually no FK2 focus and attenuated mono- and poly-ubiquitylation of γ-H2AX, following IR.[65,66] Thus, H2AX is one of substrates for Ubc13. Presumably, poly-ubiquitylation by Ubc13 modifies local chromatin structure at the site of DSB, and thus increases the accessibility of HR factors including RPA and Rad51. It is of interest whether proteolytic degradation mediated by proteasome and poly-ubiquitylation via lysine 48 (K48) is involved in this Ubc13-dependent pathway. Murakawa et al. analyzed the effect of proteasome inhibitors on DSB repair. Interestingly, treatment of the cells with proteasome inhibitors resulted in phenotypes very similar to those caused by Ubc13 deficiency including the compromised HR and the impaired recruitment of Rad51 and RPA. Thus, the ubiquitin-proteasome system plays a critical role in HR-mediated DSB repair.[67] It should be noted that Ubc13 catalyzes K63-dependent ubiquitylation implicated in signal transduction but not proteosome-mediated degradation. Thus, the relationship between Ubc13 mediated ubiquitylation and proteosome is not necessarily straightforward. Alternatively, it is possible that the proteasome inhibitors reduce free ubiquitin available for conjugation so that cells are unable to perform HR involving ubiquitylation. In summary, Ubc13-dependent ubiquitylation and probably proteolytic degradation are critical for promoting HR, which requires free singlle-stranded DNA tails, because the genome DNA of higher eukaryotic cells is maintained in a highly condensed chromatin folded into a higher order structure (Fig. 6).

7. RAD51 foci and ATM-dependent DNA damage signaling

DSBs induced by ionizing radiation are well known to stimulate the ATM-dependent DNA damage checkpoint pathway.[2] The factors involved in this pathway, such as phosphorylated ATM, form discrete foci at the sites of DSBs, which amplify DNA damage signals.[68] DSBs are repaired by two major repair pathways, NHEJ and HR.[1] Although the factors regulating NHEJ do not form foci in G1, phosphorylated ATM forms foci, and number of which correlates well with the estimated number of DNA double strand breaks. NBS1, involved in HR, has been shown to form foci, and both NBS1 and phosphorylated NBS1 foci are colocalized with phosphorylated ATM foci in G1, S and G2. In contrast to NBS1, little is known about the role of the foci of RAD51, which is the major player in HR and DNA damage checkpoint signalling. The present study examined spatiotemporal relationship between ATM foci and RAD51 foci in normal human diploid cells exposed to X-rays.

By using extensive extraction prior to fixation, we successfully detected RAD51 foci in normal human cells even 30 minutes after X-irradiation with 0.5 Gy (Fig. 7). These foci were mainly observed in the S phase cells, and most of the foci were colocalized with phosphorylated ATM foci. Interestingly, a significant change in the size of phosphorylated ATM was observed, and grown foci were colocalized with phosphorylated NBS1 and phosphorylated BRCA1 foci, while the size of RAD51 foci remained unchanged. Three dimensional analysis revealed that RAD51 foci were included in a part of the large colocalized foci. Thus, it is indicated that phosphorylated ATM foci were created and grew to encircle RAD51 foci, which are the landmarks of chromatin regions processing HR.

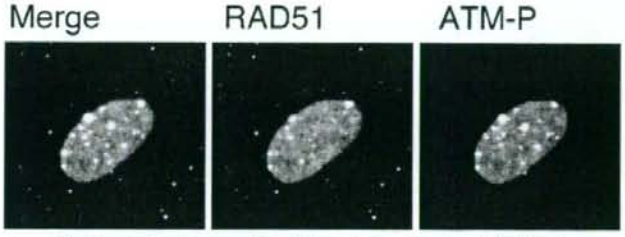

Fig. 7. Colocalization of RAD51 and phosphorylated ATM foci.

These results suggest that the DNA damage checkpoint pathway is activated not only at the sites of DNA damage repaired by NHEJ, but also at the sites processed by HR. In addition, these results indicate that the foci of DNA damage checkpoint factors do not always reflect the sites of DSB repair. Instead, they light up the chromatin regions either directly modified by DSBs, or indirectly altered through DNA repair processes. These secondary changes in the chromatin structure may be involved in amplification of DNA damage checkpoint signals.[69]

8. PERSPECTIVES

Both the HR and NHEJ repair pathways are biologically essential mechanisms for maintenance of chromosome or gene structure in higher eukaryotes. For mammalian immune systems, NHEJ is the central pathway for V(D)J recombination and HR mediates class switching.[70] Because genetic disorders accompanying compromised HR function often presents cancer predisposition, normal HR should be an absolutely error-free repair pathway. Recently, it was reported that generation of DSBs associated with DNA replication stresses such as stalled replication forks closely related to cancer incidences and that these DNA replication-related DSBs are repaired through the HR pathway.[71] This finding suggests the importance of HR repair for cancer prevention. In contrast, failure in regulation of HR often causes chromosomal translocation such as t (7:14) at TCR loci in AT patients,[72] suggesting that the HR pathway also has potential risk of genetic alteration during DSB end processing.

It is still unclear how much NHEJ pathway is error prone. After DNA resection by RAG 1/2, NHEJ proteins in V(D)J recombination somehow 'accurately' join the DNA ends although terminal deoxynucleotidyl transferase inserts additional sequences at a cording joint.[70] This suggests that the majority of DNA ends could be accurately rejoined by NHEJ. One of the reasons why the NHEJ is thought to be error prone is because the chemical structure of radiation-induced DSB ends varies and those ends are often devoid of 5'-phosphate and/or 3'-OH groups. Accordingly, these abnormal ends must be removed by a nuclease for subsequent ligation. This end processing could result in a loss of several bases adjacent to the break point. Establishment of a quantitative assay that enables us to assess both the yield of different types of radiation-induced DSB ends and the efficiency of 'accurate' end processing should be helpful to solve the raised question.

Nuclear foci formation is also a mystery of DNA damage response. It is not well understood, in spite of intensive investigation by many researchers, why such many molecules must localize at the damaged site. It is no doubt that the foci, which are formed immediately after irradiation, must be the exact sites of DNA damage and repair reactions. The majority of the known foci-forming proteins are related to HR pathway whereas none of NHEJ-functioning proteins are reported to form the radiation-induced nuclear foci. Although the phosphorylation foci of DNA-PKcs following DNA damage induction is reported,[73] this may not be *bona fide* nuclear foci formed via relocalization of the protein molecule itself. These observations suggest that the early nuclear foci could be sites of HR-repair.

In contrast to early nuclear foci, what is the biological function of the foci remaining for long time after DNA damage induction? Although it is suggested that these foci are sites of chromatin remodeling, almost all the DSBs disappear within several hours after irradiation. Thus, it is not clear why the chromatin remodeling sites persist long after the completion of DNA repair reaction. Further analysis of the mechanism of protein relocalization and chromatin remodeling would dissolve the mystery.

ACKNOWLEDGEMENTS

This review records presentations in the workshop at 50th Annual Meeting of Japan Radiation Research Society, Chiba, 2007. The authors are grateful to Drs. Yoshiya Furusawa and Koichi Ando at the National Institute for Radiological Science, Chiba, for giving us an opportunity to present our recent results in the 50th Annual Meeting of the Japan Radiation Research Society. Authors for each chapter are HT (chapters 1 and 8). KI (chapter 2), JK (chapters 3 and 8), KM (chapter 4), MT (chapter 5), ES (chapter 6), and KS (chapter 7).

REFERENCES

1. Wyman, C. and Kanaar, R. (2006) DNA double-strand break repair: All's well that ends well. Ann. Rev. Genet. **40**: 363–383.
2. Lavin, M. F. and Kozlov, S. (2007) ATM activation and DNA damage response. Cell Cycle **6**: 931–942.
3. Zhou, B-B. S. and Elledge, S. J. (2000) The DNA damage response: putting checkpoints in perspective. Nature **408**: 433–439.
4. Shiloh, Y. (2003) ATM and related protein kinases: safeguarding genome integrity. Nat. Rev. Cancer **3**: 155–168.
5. Iwabuchi, K., Bartel, P. L., Li, B., Marraccino, R. and Fields, S. (1994) Two cellular proteins that bind to wild-type but not mutant p53. Proc. Natl. Acad. Sci. USA. **91**: 6098–6102.
6. Iwabuchi, K., Li, B., Massa, H. F., Trask, B. J., Date, T. and S. Fields, S. (1998) Stimulation of p53-mediated transcriptional activation by the p53-binding proteins, 53BP1 and 53BP2. J. Biol. Chem. **273**: 26061–26068.
7. Joo, W. S., Jeffrey, P. D., Cantor, S. B., Finnin, M. S., Livingston, D. M. and Pavletich N. P. (2002) Structure of the 53BP1 BRCT region bound to p53 and its comparison to the Brca1 BRCT structure. Genes Dev. **16**: 583–593.
8. Derbyshire, D. J., Basu, B. P., Serpell, L. C., Joo, W. S., Date, T., Iwabuchi, K. and Doherty, A. J. (2002) Crystal structure of human 53BP1 BRCT domains bound to p53 tumour suppressor. EMBO J. **21**: 3863–3872.
9. Schultz, L. B., Chehab, N. H., Malikzay, A. and Halazonetis, T. D. (2000) p53-binding protein 1 (53BP1) is an early participant in the cellular response to DNA double-strand breaks. J. Cell Biol. **151**: 1381–1390.
10. Rappold, I., Iwabuchi, K., Date, T. and Chen, J. (2001) Tumor suppressor p53 binding protein 1 (53BP1) is involved in DNA damage-signaling pathways. J. Cell Biol. **153**: 613–620.
11. Charier, G., Couprie, J., Alpha-Bazin, B., Meyer, V., Quéméneur, E., Guérois, R., Callebaut, I., Gilquin, B. and Zinn-Justin, S. (2004) The Tudor tandem of 53BP1: a new structural motif involved in DNA and RG-rich peptide binding. Structure **12**:1551–1562.
12. Huyen, Y., Zgheib, O., Ditullio, R. A. Jr., Gorgoulis, V. G., Zacharatos, P., Petty, T. J., Sheston, E. A., Mellert, H. S., Stavridi, E. S. and Halazonetis, T. D. (2004) Methylated lysine 79 of histone H3 targets 53BP1 to DNA double-strand breaks. Nature **432**: 406–411.
13. Sanders, S. L., Portoso, M., Mata, J., Bähler, J., Allshire, R. C. and Kouzarides, T. (2004) Methylation of histone H4 lysine 20 controls recruitment of Crb2 to sites of DNA damage. Cell **119**: 603–614.
14. Xia, Z., Morales, J. C., Dunphy, W. G. and Carpenter, P. B. (2000) Negative cell cycle regulation and DNA-damage inducible phosphorylation of the BRCT protein 53BP1. J. Biol. Chem. **276**: 2708–2718.
15. Anderson, L., Henderson, C. and Adachi, Y. (2001) Phosphorylation and rapid relocalization of 53BP1 to nuclear foci upon DNA damage. Mol. Cell. Biol. **21**: 1719–1729.
16. Wang, B., Matsuoka, S., Carpenter, P. B. and Elledge, S. J. (2002) 53BP1, a mediator of the DNA damage checkpoint. Science **298**: 1435–1438.
17. DiTullio, R. A., Mochan, T. A., Venere, M., Barrtkova, J., Sehested, M., Bartek, J. and Halazonetis, T. D. (2002) 53BP1 functions in an ATM-dependent checkpoint pathway that is constitutively activated in human cancer. Nat. Cell Biol. **12**: 998–1002.
18. Fernandez-Capetillo, O., Chen, H. T., Celeste, A., Ward, I., Romanienko, P. J., Morales, J. C., Naka, K., Xia, Z., Camerini-Otero, R. D., Motoyama, N., Carpenter, P. B., Bonner, W. M., Chen, J. and Nussenzweig, A. (2002) DNA damage-induced G2/M checkpoint activation by histone H2AX and 53BP1. Nat. Cell Biol. **12**: 993–997.
19. Iwabuchi, K., Piku-Basu, B., Kysela, B., Kurihara, T., Shibata, M., Guan, D., Cao, Y., Hamada, T., Imamura, K., Jeggo, P. A., Date, T. and Doherty, A. J. (2003) Potential role for 53BP1 in DNA end-joining repair through direct interaction with DNA. J. Biol. Chem. **278**: 36487–36495.
20. Jackson, S. P. (2002) Sensing and repairing DNA double-strand breaks. Carcinogenesis **23**: 687–696.
21. Jeggo, P. A. (1998) DNA breakage and repair. Adv. Genet. **38**: 185–211.
22. Rothkamm, K., Kruger, I., Thompson, L. H. and Lobrich, M. (2003) Pathways of DNA double-strand break repair during the mammalian cell cycle. Mol. Cell. Biol. **23**: 5706–5715.
23. Riballo, E., Kuhne, M., Rief, N., Doherty, A., Smith, G. C., Recio, M. J., Reis, C., Dahm, K., Fricke, A., Krempler, A., Parker, A. R., Jackson, S. P., Gennery, A., Jeggo, P. A. and Löbrich, M. (2004) A pathway of double-strand break rejoining dependent upon ATM, Artemis, and proteins locating to γ-H2AX foci. Mol. Cell **16**: 715–724.
24. Iwabuchi, K., Hashimoto, M., Matsui, T., Kurihara, T., Shimizu, H., Adachi, N., Ishiai, M., Yamamoto, K., Tauchi, H., Takata, M., Koyama, H. and Date, T. (2006) 53BP1 contributes to survival of cells irradiated with X-ray during G1 without Ku70 or Artemis. Genes Cells **11**: 935–948.
25. Manis, J. P., Morales, J. C., Xia, Z., Kutok, J. L., Alt, F. W. and Carpenter, P. B. (2004) 53BP1 links DNA damage-response pathway to immunoglobulin heavy chain class-switch recombination. Nat. Immunol. **5**: 481–487.
26. Ward, I. M., Reina-San-Martin, B., Olaru, A., Minn, K., Tamada, K., Lau, J. S., Cascalho, M., Chen, L., Nussenzweig, A., Livak, F., Nussenzweig, M. C. and Chen, J. (2004) 53BP1 is required for class switch recombination. J. Cell Biol. **165**: 459–464.
27. Petersen, S., Casellas, R., Reina-San-Martin, B., Chen, H. T., Difilippantonio, M. J., Wilson, P. C., Hanitsch, L., Celeste, A., Muramatsu, M., Pilch, D. R., Redon, C., Ried, T., Bonner, W. M., Honjo, T., Nussenzweig, M. C. and Nussenzweig, A. (2001) AID is required to initiate Nbs1/γ-H2AX focus formation and mutations at sites of class switching. Nature **414**: 660–665.
28. Kobayashi, J., Antoccia, A., Tauchi, H., Matsuura, S., Komatsu, K. (2004) NBS1 and its functional role in the DNA damage response. DNA Repair **3**: 855–861.
29. Bakkenist, C. J. and Kastan, M. B. (2003) DNA damage activates ATM through intermolecular autophosphorylation and dimer dissociation. Nature **421**: 499–506.
30. Tauchi, H., Kobayashi, J., Morishima, K., van Gent, D. C.,

Shiraishi, T., Verkaik, N. S., vanHeems, D., Ito, E., Nakamura, A., Sonoda, E., Takata, M., Takeda, S., Matsuura, S. and Komatsu, K. (2002) Nbs1 is essential for DNA repair by homologous recombination in higher vertebrate cells. Nature **420**: 93–98.
31. Kobayashi, J., Tauchi, H., Sakamoto, S., Nakamura, A., Morishima, K., Matsuura, S., Kobayashi, T., Tamai, K., Tanimoto, K. and Komatsu, K. (2002) NBS1 Localizes to γ-H2AX Foci through Interaction with the FHA/BRCT Domain. Current Biol. **12**: 1846–1851.
32. Sakamoto, S., Iijima, K., Mochizuki, D., Nakamura, K., Teshigawara, K., Kobayashi, J., Matsuura, S., Tauchi, H. and Komatsu, K. (2007) Homologous recombination repair is regulated by domains at the N- and C-terminus of NBS1 and is dissociated with ATM functions. Oncogene **26**: 6002–6009.
33. Uchimura, Y., Nakamura, M., Sugasawa, K., Nakao, M. and Saitoh, H. (2004) Overproduction of eukaryotic SUMO-1- and SUMO-2-conjugated proteins in Escherichia coli. Anal. Biochem. **331**: 204–206.
34. Osman, F. and Whitby, M. C. (2007) Exploring the roles of Mus81-Eme1/Mms4 at perturbed replication forks. DNA Repair **6**: 1004–1017.
35. Doe, C. L., Ahn, J. S., Dixon, J. and Whitby, M. C. (2002) Mus81-Eme1 and Rqh1 involvement in processing stalled and collapsed replication forks. J. Biol. Chem. **277**: 32753–32759.
36. Abraham, J., Lemmers, B., Hande, M. P., Moynahan, M. E., Chahwan, C., Ciccia, A., Essers, J., Hanada, K., Chahwan, R., Khaw, A. K., McPherson, P., Shehabeldin, A., Laister, R., Arrowsmith, C., Kanaar, R., West, S. C., Jasin, M. and Hakem, R. (2003) Eme1 is involved in DNA damage processing and maintenance of genomic stability in mammalian cells. EMBO J. **22**: 6137–6147.
37. Dendouga, N., Gao, H., Moechars, D., Janicot, M., Vialard, J. and McGowan, C. H. (2005) Disruption of murine Mus81 increases genomic instability and DNA damage sensitivity but does not promote tumorigenesis. Mol. Cell. Biol. **25**: 7569–7579.
38. Hiyama, T., Katsura, M., Yoshihara, T., Ishida, M., Kinomura, A., Tonda, T., Asahara, T. and Miyagawa, K. (2006) Haploinsufficiency of the Mus81-Eme1 endonuclease activates the intra-S-phase and G2/M checkpoints and promotes rereplication in human cells. Nucleic Acids Res. **34**: 880–892.
39. McPherson, J. P., Lemmers, B., Chahwan, R., Pamidi, A., Migon, E., Matysiak-Zablocki, E., Moynahan, M. E., Essers, J., Hanada, K., Poonepalli, A., Sanchez-Sweatman, O., Khokha, R., Kanaar, R., Jasin, M., Hande, M. P. and Hakem R. (2004) Involvement of mammalian Mus81 in genome integrity and tumor suppression. Science **304**: 1822–1826.
40. Pamidi, A., Cardoso, R., Hakem, A., Matysiak-Zablocki, E., Poonepalli, A., Tamblyn, L., Perez-Ordonez, B., Hande, M. P., Sanchez, O. and Hakem, R. (2007) Functional interplay of p53 and Mus81 in DNA damage responses and cancer. Cancer Res. **67**: 8527–8535.
41. Wang, W. (2007) Emergence of a DNA-damage response network consisting of Fanconi anaemia and BRCA proteins. Nat. Rev. Genet. **8**: 735–748.
42. Sasaki, M. S. and Tonomura, A. (1973) A high susceptibility of Fanconi's anemia to chromosome breakage by DNA cross-linking agents. Cancer Res. **33**: 1829–1836.
43. Takata, M., Sasaki, M. S., Sonoda, E., Fukushima, T., Morrison, C., Albala, J. S., Swagemakers, S. M., Kanaar, R., Thompson, L. H. and Takeda, S. (2000) The Rad51 paralog Rad51B promotes homologous recombinational repair. Mol. Cell. Biol. **20**: 6476–6482.
44. Takata, M., Sasaki, M. S., Tachiiri, S., Fukushima, T., Sonoda, E., Schild, D., Thompson, L. H. and Takeda, S. (2001) Chromosome instability and defective recombinational repair in knockout mutants of the five Rad51 paralogs. Mol. Cell. Biol. **21**: 2858–2866.
45. Venkitaraman, A. R. (2002) Cancer susceptibility and the functions of BRCA1 and BRCA2. Cell **108**: 171–182.
46. Taniguchi, T., Garcia-Higuera, I., Andreassen, P. R., Gregory, R. C., Grompe, M. and D'Andrea, A. D. (2002) S-phase-specific interaction of the Fanconi anemia protein, FANCD2, with BRCA1 and RAD51. Blood **100**: 2414–2420.
47. Garcia-Higuera, I., Taniguchi, T., Ganesan, S., Meyn, M. S., Timmers, C., Hejna, J., Grompe, M. and D'Andrea, A. D. (2001) Interaction of the Fanconi anemia proteins and BRCA1 in a common pathway. Mol. Cell **7**: 249–262.
48. Seki, S., Ohzeki, M., Uchida, A., Hirano, S., Matsushita, N., Kitao, H., Oda, T., Yamashita, T., Kashihara, N., Tsubahara, A., Takata, M. and Ishiai, M. (2007) A requirement of FancL and FancD2 monoubiquitination in DNA repair. Genes Cells **12**: 299–310.
49. Takata, M., Kitao, H. and Ishiai, M. (2007) Fanconi anemia: genetic analysis of a human disease using chicken system. Cytogenet. Genome Res. **117**: 346–351.
50. Yamamoto, K., Ishiai, M., Matsushita, N., Arakawa, H., Lamerdin, J. E., Buerstedde, J. M., Tanimoto, M., Harada, M., Thompson, L. H. and Takata, M. (2003) Fanconi anemia FANCG protein in mitigating radiation- and enzyme-induced DNA double-strand breaks by homologous recombination in vertebrate cells. Mol. Cell. Biol. **23**: 5421-5430.
51. Yamamoto, K., Hirano, S., Ishiai, M., Morishima, K., Kitao, H., Namikoshi, K., Kimura, M., Matsushita, N., Arakawa, H., Buerstedde, J. M., Komatsu, K., Thompson, L. H. and Takata, M. (2005) Fanconi anemia protein FANCD2 promotes immunoglobulin gene conversion and DNA repair through a mechanism related to homologous recombination. Mol. Cell. Biol. **25**: 34–43.
52. Arakawa, H. and Buerstedde, J. M. (2004) Immunoglobulin gene conversion: Insights from bursal B cells and the DT40 cell line. Dev. Dyn. **229**: 458–464.
53. Buerstedde, J. M., Reynaud, C. A., Humphries, E. H., Olson, W., Ewert, D. L. and Weill, J. C. (1990) Light chain gene conversion continues at high rate in an ALV-induced cell line. EMBO J. **9**: 921–927.
54. Takata, M., Sasaki, M. S., Sonoda, E., Morrison, C., Hashimoto, M., Utsumi, H., Yamaguchi-Iwai, Y., Shinohara, A. and Takeda, S. (1998) Homologous recombination and non-homologous end-joining pathways of DNA double-strand break repair have overlapping roles in the maintenance of chromosomal integrity in vertebrate cells. EMBO J. **17**: 5497–5508.
55. Ira, G., Pellicioli, A., Balijja, A., Wang, X., Fiorani, S.,

Carotenuto, W., Liberi, G., Bressan, D., Wan, L., Hollingsworth, N. M., Haber, J. E. and Foiani, M. (2004) DNA end resection, homologous recombination and DNA damage checkpoint activation require CDK1. Nature **431**: 1011–1017.

56. Limbo, O., Chahwan, C., Yamada, Y., de Bruin, R. A., Wittenberg, C. and Russell, P. (2007) Ctp1 is a cell-cycle-regulated protein that functions with Mre11 complex to control double-strand break repair by homologous recombination. Mol. Cell **28**: 134–146.
57. Sartori, A. A., Lukas, C., Coates, J., Mistrik, M., Fu, S., Bartek, J., Baer, R., Lukas, J. and Jackson, S. P. (2007) Human CtIP promotes DNA end resection. Nature **450**: 509–514.
58. Fukushima, T., Takata, M., Morrison, C., Araki, R., Fujimori, A., Abe, M., Tatsumi, K., Jasin, M., Dhar, P. K., Sonoda, E., Chiba, T. and Takeda, S. (2001) Genetic analysis of the DNA-dependent protein kinase reveals an inhibitory role of Ku in late S-G2 phase DNA double-strand break repair. J. Biol. Chem. **276**: 44413–44418.
59. Kitao, H., Yamamoto, K., Matsushita, N., Ohzeki, M., Ishiai, M. and Takata, M. (2006) Functional interplay between BRCA2/FANCD1 and FANCC in DNA repair. J. Biol. Chem. **281**: 21312–21320.
60. Takata, M., Yamamoto, K., Matsushita, N., Kitao, H., Hirano, S. and Ishiai, M. (2006) The fanconi anemia pathway promotes homologous recombination repair in DT40 cell line. Subcell Biochem **40**: 295–311.
61. Kannouche, P. L., Wing, J. and Lehmann, A. R. (2004). Interaction of human DNA polymerase eta with monoubiquitinated PCNA: a possible mechanism for the polymerase switch in response to DNA damage. Mol. Cell **14**: 491–500.
62. Watanabe, K., Tateishi, S., Kawasuji, M., Tsurimoto, T., Inoue, H. and Yamaizumi, M. (2004). Rad18 guides poleta to replication stalling sites through physical interaction and PCNA monoubiquitination. EMBO J. **23**: 3886–3896.
63. Deng, L., Wang, C., Spencer, E., Yang, L., Braun, A., You, J., Slaughter, C., Pickart, C. and Chen, Z. J. (2000). Activation of the IkappaB kinase complex by TRAF6 requires a dimeric ubiquitin-conjugating enzyme complex and a unique polyubiquitin chain. Cell **103**: 351–361.
64. Spence, J., Gali, R. R., Dittmar, G., Sherman, F., Karin, M. and Finley, D. (2000). Cell cycle-regulated modification of the ribosome by a variant multiubiquitin chain. Cell **102**: 67–76.
65. Zhao, G. Y., Sonoda, E., Barber, L. J., Oka, H., Murakawa, Y., Yamada, K., Ikura, T., Wang, X., Kobayashi, M., Yamamoto, K., Boulton, S. J. and Takeda, S. (2007). A Critical Role for the Ubiquitin-Conjugating Enzyme Ubc13 in Initiating Homologous Recombination. Mol. Cell **25**: 663–675.
66. Ikura, T., Tashiro, S., Kakino, A., Shima, H., Jacob, N., Amunugama, R., Yoder, K., Izumi, S., Kuraoka, I., Tanaka, K., Kimura, H., Ikura, M., Nishikubo, S., Ito, T., Muto, A., Miyagawa, K., Takeda, S., Fishel, R., Igarashi, K. and Kamiya, K. (2007). DNA damage-dependent acetylation and ubiquitination of H2AX enhances chromatin dynamics. Mol. Cell Biol. **27**: 7028–7040.
67. Murakawa, Y., Sonoda, E., Barber, L. J., Zeng, W., Yokomori, K., Kimura, H., Niimi, A., Lehmann, A., Zhao, G. Y., Hochegger, H., Boulton, S. J. and Takeda, S. (2007). Inhibitors of the proteasome suppress homologous DNA recombination in Mammalian cells. Cancer Res. **67**: 8536–8543.
68. Suzuki, K., Okada, H., Yamauchi, M., Oka, Y., Kodama, S. and Watanabe, M. (2006) Qualitative and quantitative analysis of phosphorylated ATM foci induced by low-dose ionizing radiation. Radiat. Res. **165**: 499–504.
69. Downs, J. A., Nussenzweig, M. C. and Nussenzweig, A. (2007) Chromatin dynamics and the preservation of genetic information. Nature 447: 951–958.
70. Lieber, M. R., Ma, Y., Pannicke, U. and Schwarz, K. (2004) The mechanism of vertebrate nonhomologous DNA end joining and its role in V(D)J recombination. DNA Repair **3**: 817–826.
71. McCabe, N., Turner, N. C., Lord, C. J., Kluzek, K., Bialkowska, A., Swift, S., Giavara, S., O'Connor, M. J., Tutt, A. N., Zdzienicka, M. Z., Smith, G. C. and Ashworth, A. (2006) Deficiency in the repair of DNA damage by homologous recombination and sensitivity to poly(ADP-ribose) polymerase inhibition. *Cancer Res.* **66**: 8109–8115.
72. Tauchi, H., Matsuura, S., Kobayashi, J., Sakamoto, S. and Komatsu, K. (2002) Nijmegen breakage syndrome gene, NBS1, and molecular links to factors for genome stability. *Oncogene* **21**: 8967–8680.
73. Chan, D. W., Chen, B. P., Prithivirajsingh, S., Kurimasa, A., Story, M. D., Qin, J. and Chen, D. J. (2002) Autophosphorylation of the DNA-dependent protein kinase catalytic subunit is required for rejoining of DNA double-strand breaks. *Genes Dev.* **16**: 2333–2338.

Received on December 26, 2007
Revision received on January 14, 2008
Accepted on January 15, 2008
J-STAGE Advance Publication Date: February 19, 2008